increasingly important. We have previously reported the intrafraction motion of the pancreas using the Calypso System in patients with unresectable pancreatic cancer. The present study reports interfraction motion using the Calypso System.

Materials/Methods: Calypso Beacon transponders were implanted into pancreatic cancer patients for tumor tracking during daily setup and radiation delivery. Transponders were placed during routine exploratory laparoscopy performed to rule out peritoneal metastasis. Under laparoscopic guidance, 3 transponders were implanted in a triangulated fashion into the pancreas. All patients underwent a free-breathing "slow scan" for CT based planning to control for centroid motion. Patients were initially positioned for radiation treatment using skin tattoos and orthogonal port films. The patients were then shifted from their initial position based on localization information from the Calypso System to position the tumor centroid between the maxima and minima of oscillation. Interfraction motion was evaluated in the left-right (X), superior-inferior (Y), and anterior-posterior dimensions (Z). Calypso patient set-up data was collected for 164 consecutive treatment sessions.

Results: The median initial shift from tattoos and orthogonal films based on the Calypso System was less than 0.5 cm for all three dimensions. Based on the 164 shifts, the mean shift in cm for the X, Y and Z dimensions were -0.18, 0.27, and -0.32, respectively. The median X, Y, and Z shifts in cm (followed by SD in parenthesis) were -0.06 (0.72), 0.11 (0.85), and -0.30 (0.41).

Conclusions: At present a 1.5-2.0 cm PTV is added to the CTV at our institution when treating pancreatic cancer definitively. Based on the Calypso System data examined here, it appears that this is adequate. The SDs of the shifts suggest that a PTV of 2 cm would account for the majority of interfractional motion when only skin marks and orthogonal films are used. This margin would also be adequate to account for intrafraction motion, which was much greater, based on previously reported data. The use of the Calypso system may allow smaller margins to be used, which may allow physicians greater flexibility in choosing treatments for patients, such as using hypofractionated radiation or higher doses of chemotherapy. While this data is preliminary, it is encouraging and warrants further study.

Author Disclosure: E.T. Shinohara, Honoraria, D. Speakers Bureau/Honoraria; A. Kassaee, None; N. Vapiwala, Honoraria, D. Speakers Bureau/Honoraria; J. Plastaras, None; J. Drebin, None; J. Metz, Honoraria, D. Speakers Bureau/Honoraria.

3069 Interfractional Variations of Lung Tumor in the Stereotactic Body Radiotherapy with Cine EPID at Treatment

Y. Ueda, K. Tsujii, K. Shirai, M. Miyazaki, K. Miyagi, O. Suzuki, K. Nishiyama

Osaka Medical Center for Cancer, Osakashi, Japan

Purpose/Objective(s): At stereotactic radiotherapy (SBRT) for lung cancer, errors in patient set-up and changes of tumor motion are two major interfractional variations. We evaluated these variations using an electronic portal imaging device (EPID) in cine mode during treatment.

Materials/Methods: The subjects were 33 patients with stage I non-small lung cancer treated with SBRT at our institution. Simulation processes included respiratory correlated 4 dimensional CT (4D-CT) and a Varian Real-Time Position Management system. 4D-CT data were divided into 10 respiratory phases and reformed into the maximum intensity (MIP) and averaged intensity projection images (AVE-IP). Internal target volume (ITV) was defined as a tumor shadow on MIP images. Peak-to-peak movement (M-4D-CT) was measured using 10 bins of 4D-CT and the coordinate of the tumor geometrical center on AVE-IP was calculated (mean tumor position on AVE-IP: MTP-AVE). At every treatment, a cone-beam CT (CBCT) scan was acquired before irradiation. CBCT and AVE-IP images were registered according to tumor shadow to each other by viewing three planes (axial, sagittal and coronal) for patient positioning. At 3 sessions of every patient, tumor shadows were acquired on anterior-posterior images of an electronic portal imaging device (EPID) in cine mode at 2 frames per second. Using an in-house template matching software, the geometric center of the tumor was demonstrated on each cine EPID image and its trajectory was drawn. The motion length (M-Cine) and the average coordinate (MTP-Cine) of the geometrical center were derived from the trajectory. The differences between M-4D-CT and M-Cine and between MTP-AVE and MTP-Cine along the cranio-caudal direction were estimated as interfractional variations of tumor motion change and patient setup error, respectively.

Results: M-4D-CT (mean ± SD) was 3.3 ± 3.5 mm (range: 0-16.3 mm) and M-Cine was 4.2 ± 3.8 mm (range: 0.3-16.4 mm). The differences of absolute values between M-4D-CT and M-Cine and between MTP-AVE and MTP-Cine were 1.4 ± 1.4 mm (mean ± SD) and 1.4 ± 1.8 mm, respectively. The increases in M-Cine from M-4D-CT and the shift of MTP-Cine from MTP-AVE were less than 3 mm in 90% and 95% of all sessions, respectively.

Conclusions: Considering both interfractional variations of tumor motion changes (M-4D-CT vs. M-Cine) and mean tumor positions (MTP-AVE vs. MTP-Cine), the total margin added to ITV to make PTV was calculated at 6 mm using the formula described by Stroom *et al.*

Author Disclosure: Y. Ueda, None; K. Tsujii, None; K. Shirai, None; M. Miyazaki, None; K. Miyagi, None; O. Suzuki, None; K. Nishiyama, None.

3070 A Novel Markerless Technique to Evaluate Daily Lung Tumor Motion

Y. Yang[1], Z. Zhong[1], X. Guo[1], J. Anderson[2], T. Solberg[2], W. Mao[2]

[1]University of Texas at Dallas, Richardson, TX, [2]University of Texas Southwestern Medical Center at Dallas, Dallas, TX

Purpose/Objective(s): Cone-beam CT (CBCT) has been widely used to localize patients for radiation therapy, particularly for Stereo Body Radiation Therapy (SBRT) lung cancer treatment. In planning for lung SBRT, 4D-CT is often used to derive patient-specific clinical target (CTV) and planning target (PTV) volumes. Other motion management techniques such as abdominal compression may also be used to reduce respiratory motion. Motion characteristics at the time of treatment, however, can differ significantly from those determined by 4D-CT. The use of 4D CBCT to address this issue is

2706 Feasibility and Toxicity of Dose-Escalated 4D Adaptive Image-guided Radiotherapy (IGRT) for Non-small Cell Lung Cancer (NSCLC)

M. C. McGee, I. S. Grills, D. Ionascu, J. Wloch, S. Martin, J. Margolis, R. Welsh, G. Chmielewski, D. Yan, L. L. Kestin

William Beaumont Hospital, Royal Oak, MI

Purpose/Objective(s): To report technique, feasibility, and toxicity of hyperfractionated accelerated 4D IGRT for NSCLC.

Materials/Methods: Seventeen patients with clinical stage III NSCLC were treated on a phase I/II protocol at William Beaumont Hospital (2008-2010). A 4D CT (10 phases) and ^{18}FDG-PET were acquired and fused for planning. All clinical data was used to define known disease (GTV). Phase 1 of the 4D CT was used for GTV and normal structure contours, which were propagated to create an ITV of the primary tumor and average normal structure volumes. $CTV_{primary}$ was defined as a 5 mm 3D expansion of the $ITV_{primary}$. CTV_{nodal}=GTV_{nodal}. PTV=CTV + 5 mm. In the preoperative setting, objective dose was 54 Gy in 1.5 Gy fractions BID to PTV D99. For definitive RT, initial objective dose was 66 Gy with dose escalation to 72 Gy in 1.5 Gy fractions BID (5 days per week). Intensity-modulated RT was utilized for all cases to achieve adequate dosimetric coverage and normal tissue constraints. If constraints prevented delivery of the intended PTV dose, only the maximum allowable dose was prescribed while still meeting all constraints. On-line CBCT IGRT was performed for each fraction with registration performed based on optimal alignment of both $PTV_{primary}$ and PTV_{nodal}. Toxicities were scored utilizing CTC v 3.0.

Results: Seventeen patients were treated with median follow-up of 1.0 year. Mean age was 63.8 years. 11 patients (65%) were stage IIIA and 6 patients (35%) were stage IIIB. 3 were stage N3, 13 were N2, and 1 T4N0. 82% had adenocarcinoma, 12% squamous, and 6% large cell carcinoma. All patients completed the prescribed dose of RT with a median dose of 66 Gy (mean 64.2 Gy) in a median of 44 fractions (mean 42.8) over a median of 31 elapsed days. Three stage IIIA patients were treated preoperatively to 54 Gy. Definitive chemo-RT cases received 60 Gy (n = 2), 63 Gy (n = 2), 66 Gy (n = 6), and 72 Gy (n = 4). All received concurrent chemotherapy (82% cisplatin/etoposide, 12% carboplatin/taxol, 6% carboplatin/etoposide). 3 patients (17%) developed ≥ grade 2 (G2) pneumonitis (at 3 and 6 months) and 1 (6%) had ≥ grade 3 (G3) pneumonitis 6 months after RT. 6 patients developed acute G2 esophagitis. 1 patient (6%) had chronic G2 esophagitis at 12 months after RT. 2 patients (12%) had acute G2 myositis with no chronic G2 myositis reported. The 1-year rate for local recurrence was 6%, regional recurrence 30%, and distant metastasis 31%. Only one patient died (with distant metastasis) for a 1-year overall survival of 92%.

Conclusions: Dose-escalated hyperfractionated accelerated RT using a 4D adaptive approach with online image guidance and concurrent chemotherapy is a feasible treatment for NSCLC with acceptable acute and chronic toxicity with promising early data in this prospective series.

Author Disclosure: M.C. McGee, None; I.S. Grills, None; D. Ionascu, None; J. Wloch, None; S. Martin, None; J. Margolis, None; R. Welsh, None; G. Chmielewski, None; D. Yan, None; L.L. Kestin, None.

2707 Radiotherapy for the Second Lung Mass after Surgical Resection of the First Lung Cancer

K. Miyagi, A. Nakajima, Y. Kawaguchi, O. Suzuki, S. Nakamura, K. Nishiyama

Osaka Medical Center for Cancer and Cardiovascular Diseases, Osaka, Japan

Purpose/Objective(s): To estimate the outcome of 3-dimensional conformal radiotherapy (3D-CRT) and stereotactic radiotherapy (SRT) for second lung tumor after resection of lung cancer.

Materials/Methods: Between March 2000 and February 2008, 3D-CRT or SRT for second lung tumor was performed in 60 patients who had undergone resection of first lung cancer (non-small cell lung cancer). According to Martini's criteria, those second lung tumors were classified into second primary lung cancer (SPLC) (50 cases) and intrapulmonary metastasis (PM) of first lung cancer (10 cases). Five patients with PM had metastasis in other sites (group A) and the other 5 did not (group B). The median interval between resection of first lung cancer and detection of second lung tumor was 40 months for SPLC (range, 11-160) and 10 months for PM (range, 4-20). Histology was adenocarcinoma in 35 patients, squamous cell carcinoma in 16 and no pathologic evidence in 9. Stage was T1 in 45 patients and T2 in 15. In SRT, total doses were 48 Gy in 4 fractions for 16 patients and 60 Gy in 10 fractions for 5. In 3D-CRT, total doses were 60-72 Gy in 10-24 fractions, 3 to 7 Gy a day, for 39 patients. The median follow-up was 32.5 months (range, 4-104).

Results: Three-year overall survival (OS) was 71% for SPLC and 60% for PM ($p = 0.43$). Three-year local control rate was 82% for SPLC and 88% for PM ($p = 0.87$). Three-year cause specific survival (CSS) was 84% for SPLC and 60% for PM ($p = 0.10$). 3-year CSS was 40% for group A of PM, which was significantly lower than that for SPLC ($p = 0.03$). However, 3-year CSS was 80% for group B of PM, which was similar to that for SPLC ($p = 0.72$). When SPLC and group B of PM were classified according to the biologically effective dose with an α/β ratio of 10 (BED_{10}), 3-year CSS was 93% for $BED_{10} > 100$ Gy and 80% for $BED_{10} < 100$ Gy. There were one case with Grade 5 radiation-induced pneumonitis and one case with Grade 3 dyspnea.

Conclusions: Radiotherapy was feasible treatment for second lung tumor after resection of first lung cancer and provided excellent prognosis especially when doses of $BED_{10} > 100$ Gy were irradiated. We suppose that SPLC and PM without any other metastasis should be aggressively treated because of their similar favorable CSS.

Author Disclosure: K. Miyagi, None; A. Nakajima, None; Y. Kawaguchi, None; O. Suzuki, None; S. Nakamura, None; K. Nishiyama, None.

2708 A Prospective Multicenter Study of Stereotactic Radiosurgery for the Treatment of Stage I NSCLC in Medically Inoperable Patients

A. Pennathur[1], R. I. Whyte[2], D. E. Heron[3], B. W. Loo[2], D. G. Brachman[4], W. E. Gooding[3], A. Zajac[5], N. A. Christie[1], H. D. Urschel[6], J. D. Luketich[1]

[1]University of Pittsburgh Medical Center, Pittsburgh, PA, [2]Stanford University School of Medicine, Stanford, CA, [3]University of Pittsburgh Cancer Institute, Pittsburgh, PA, [4]St.Joseph's Hospital and Medical Center/BNI, Phoenix, AZ, [5]St.Catherine Hospital, East Chicago, IN, [6]Baylor Medical Center, Dallas, TX

[3]Department of Surgery, Leiden University Medical Center, Leiden, Netherlands, [4]Department of Radiotherapy, Università Cattolica S. Cuore, Rome, Italy, [5]Bioimmagini e Scienze Radiologiche, Università Cattolica S.Cuore, Rome, Italy, [6]Department of Surgery, Leiden University Medical Center, Leiden, Leiden, Netherlands, [7]Department of Surgery, Uppsala University Hospital, Uppsala, Sweden, [8]Department of Radiotherapy, The Maria Sklodowska-Curie Memorial Cancer Centre, Warsaw, Poland

Purpose/Objective(s): To develop validated nomograms for accurate prediction of local recurrence (LR), distant metastases (DM) and overall survival (OS) within 5 years of follow-up for rectal cancer patients treated with short-course radiotherapy (RT) and surgery. This should allow proper selection in future trials and selection of patients who may benefit most from more intensive follow-up and postoperative treatment.

Materials/Methods: A pooled database with clinical data from three trials (1552 pts) was used for nomogram building; the Polish Rectal Cancer trial (144 pts)[1], the Swedish Rectal Cancer trial (495 pts)[2] and the Dutch TME trial (913 pts)[3]. All included patients were treated with preoperative 5 x 5 Gy RT and surgery. The relevant clinical data present in all datasets were: sex, age, tumor distance to anal verge, surgery type (TME/conventional), surgery group (local, LAR, APR), residual disease, pT-, pN- and pM-staging, overall pathological stage, radicality of the surgery and the presence of postoperative complications. A multivariate analysis (pSVM) was used to train and validate the prediction models. Performance of the model was expressed as the Area-Under-the-Curve (AUC) of the Receiver Operating Characteristic (ROC) curves. Nomograms were developed based on internal randomized validation with an optimal training set size of 60%. Logistic regression was used to convert the assigned weights of each selected predictor to a probability for 5-year outcome.

Results: The occurrences of events in the pooled database were 7.1% LR, 25.3% DM and 61.5% OS. The performance of the developed models for the validation sets were AUC_{LR} = 0.73+/-0.033 (SD), AUC_{MD} = 0.75 +/- 0.018, AUC_{OS} = 0.77+/-0.015 and consistent with the performance on the training sets. Pathological staging and residual disease were important predictors for all outcomes. Age and pN-stage were specifically predictive for DM and OS and surgery type for LR and DM.

Conclusions: The developed nomograms are able to accurately predict long-term outcome for rectal cancer patients after short-course radiotherapy and surgery and have been validated within a large pooled trial database. These nomograms should allow proper stratification in future trials and selection of patients who may benefit most from intensive follow-up and postoperative treatment.

References: [1] Bujko et al. 2005, Colorectal Disease; 7:410-416
[2] Folkesson et al. 2005, J Clin Oncol.; 23(24):5644-50
[3] Kapiteijn et al. 2001, N Engl J Med.; 345(9):638-46

Author Disclosure: R.V. Stiphout, None; W. van Gijn, None; V. Valentini, None; G. Lammering, None; M.A. Gambacorta, None; C. van de Velde, None; L. Pahlman, None; K. Bujko, None; P. Lambin, None.

1129 Combined Modality Therapy for Rectal Cancer: Analysis of Potential Differences in Disease Presentation, Treatment Adherence, and Treatment Outcome According to Race

S. Liauw[1], S. Song[1], N. Tonlaar[1], J. C. Hong[2], B. D. Minsky[1], D. T. Chang[2], B. Polite[1]

[1]University of Chicago, Chicago, IL, [2]Stanford University, Palo Alto, CA

Purpose/Objective(s): Population-based studies suggest that African Americans (AAs) with rectal cancer have a worse overall outcome compared to whites. This relationship was explored in a cohort of locally advanced rectal cancer patients treated with preoperative chemoradiation (CRT) and surgery at two urban academic cancer centers.

Materials/Methods: A total of 146 patients underwent curative-intent combined modality therapy for adenocarcinoma of the rectum. The median age was 57 years. Median dose was 50.4 Gy, given with 5-flourouracil based concurrent chemotherapy. Analysis was performed to test for differences in disease presentation, adherence to recommended therapy, and treatment outcome (freedom from failure, FFF) by race. Median follow-up was 34 months from completion of chemoRT.

Results: Twenty-six patients (18%) were AA, and 120 (82%) patients were White, Asian, or Hispanic. AA patients had longer times from diagnosis to start of therapy (median 45 days vs. 35 days, $p < 0.01$) and from CRT completion to surgery (median 42 days vs. 46 days, $p = 0.03$). CRT treatment time was no different between the two groups (median 38 days for both groups, $p = 0.53$). In the subset of patients with preoperative staging by endoscopic ultrasound (EUS, n = 119), AA patients presented with more favorable disease (20% stage I, 47% stage II, 33% stage II) compared with non-AA patients (0% stage I, 50% stage II, 48% stage III, 2% stage IV, $p < 0.01$). Among patients with stage II-IV disease (n = 116), the rate of any T or N downstaging was lower for AA patients (58% vs. 79%, $p = 0.13$). Pathologic complete response rates were also lower (17% vs. 26% for non-AA patients, $p = 0.47$), although not statistically different. AA patients were less likely to receive adjuvant chemotherapy (58% vs. 89%, $p = 0.01$). Log-rank analysis showed that time from diagnosis to therapy, and time from CRT to surgery were not associated with any difference in FFF when stratified by the median value. Similarly, completion of adjuvant chemotherapy was not associated with FFF. Overall, AA patients were not more likely to recur after therapy (FFF-3y, 100% for AA patients vs. 81% for non-AA patients, $p = 0.09$).

Conclusions: This analysis reflects differences in time from preoperative therapy to surgery and a lower rate of adjuvant therapy in AA patients with rectal cancer treated in at two urban academic cancer centers. These differences did not appear to result in inferior disease outcome for this cohort. Further study is necessary to explore the reasons underlying the delays in therapy and lower rates of adjuvant chemotherapy for AA patients.

Author Disclosure: S. Liauw, None; S. Song, None; N. Tonlaar, None; J.C. Hong, None; B.D. Minsky, None; D.T. Chang, None; B. Polite, None.

1130 Patterns of Failure in Patients with Clinical Stage IA Thoracic Esophageal Cancer treated with Definitive Radiotherapy Using Localized Field

Y. Kawaguchi, S. Nakamura, K. Miyagi, A. Nakajima, O. Suzuki, K. Nishiyama

Osaka Medical Center for Cancer & Cardiovascular Diseases, Osaka, Japan

Purpose/Objective(s): To evaluate the treatment outcome of definitive radiotherapy (RT) and patterns of the first sites of recurrence in patients with clinical stage IA thoracic esophageal carcinoma, and to determine whether elective nodal irradiation is necessary or not for these patients.

Materials/Methods: During the period from January 2000 to December 2007, 68 patients with clinical stage IA thoracic esophageal cancer, aged 43-84 years, received definitive RT. Treatment was chemoradiotherapy in 58 patients (60 Gy/30 fractions) and RT alone in 10 (8 patients ; 60 Gy/30 fractions , 2 patients ; 70 Gy/35 fractions). Concurrent chemotherapy mainly consisted of cisplatin 70 mg/m^2/day (days 1, 29) and 5-FU 700 mg/m^2/day (days 1-4, 29-32). Radiation field in this study was localized field including the primary tumor with a 3-cm margin cranio-caudally. Patterns of failure were classified according to first sites of recurrence. In-field, regional and distant lymph node recurrences were defined as lymph node failures within the irradiated area, within the mediastinum and perigastric area beyond the irradiated area and outside the regional lymph nodes, respectively.

Results: The 3-year overall survival and cause-specific survival rates were 75% and 88%, respectively, with a median follow-up of 32 months. Twenty-two of the 68 patients showed treatment failures. Of these 22, local recurrence with or without recurrence of other site, lymph node recurrence alone and distant metastasis were observed in 11, 10 and 1 patient, respectively. Of the 10 patients with lymph node recurrence alone, sites of failure were regional in 3 patients, in-field in 1, in-field and distant in 1 and distant in 5. Late toxicities occurred in 2 patients (Grade 3 and Grade 5 radiation pneumonitis in each).

Conclusions: In our study, 3 out of 68 patients developed regional lymph node recurrence alone. Considering the frequency of regional recurrence and risks of late sequelae resulting from extended field, we suppose that localized field is adequate for clinical stage IA thoracic esophageal cancer.

Author Disclosure: Y. Kawaguchi, None; S. Nakamura, None; K. Miyagi, None; A. Nakajima, None; O. Suzuki, None; K. Nishiyama, None.

1131 Incorporating SNPs as Biomarkers to Improve the Fit of the Lyman Model for Radiation Pneumonitis

Z. Liao[1], Q. Wei[1], M. K. Martel[1], D. Gomez[1], Z. Liu[1], X. Guan[2], Y. Zhuang[1], C. Lu[1], R. Komaki[1], S. L. Tucker[1]

[1]M.D. Anderson Cancer Center, Houston, TX, [2]Jinling Hospital - Nanjing University School of Medicine, Nanjing, China

Purpose/Objective(s): To test the hypothesis that the Lyman model for predicting the risk of radiation pneumonitis (RP) based on mean lung dose (MLD) can be significantly improved by incorporating biomarkers such as single nucleotide polymorphisms (SNPs) in tissue-injury and repair-related genes.

Materials/Methods: This analysis included 143 patients with non-small cell lung cancer (NSCLC) treated with definitive radiotherapy with (N = 114) or without (N = 29) concurrent chemotherapy. We genotyped 15 potentially functional SNPs (M677, MDM2_P3_TA, MTRR, XRCC3, XRCC_NCI, VEGF2061, VEGF3963, VEGF4039, TNF0629, TNF9964, TNFR622, TNFR625, TGFβ469, TGFβ073, and TGFβ471) in the genes related to DNA repair, inflammation, folic acid metabolism, and angiogenesis. The endpoint for analysis was the time to development of CTCAE grade 3 or higher RP. Using a forward stepwise procedure, candidate SNPs were added to the Lyman model based on MLD alone, with indicator variables used to represent each genotype. Genotypes occurring in 3 or fewer patients were not analyzed. The significance of improvement was assessed using the likelihood-ratio test.

Results: The parameters of the Lyman MLD model fitted to the data from this cohort were TD50 = 27.5 Gy and m = 0.42.The SNP that most significantly improved the fit of the Lyman model based on MLD alone was XRCC_NCI. Patients with XRCC_NCI = WW had an increased risk of RP with a TD50 of 21.5 Gy compared to 30.6 Gy for patients with the PP or PW genotype ($p = 0.013$). Inclusion of the VEGF4039 SNP further improved the model fit ($p = 0.035$), with the CT/TT genotypes conferring increased risk of RP. Patients with XRCC_NCI = WW and VEGF4039 = CT/TT had a TD50 only half as large (16.7 Gy) as patients with XRCC_NCI = PP/PW and VEGF4039 = CC (33.8 Gy). The model was further improved with inclusion of TNF0629 = AA as a risk factor ($p = 0.048$), although there were only 4 patients with this genotype. The SNP previously identified by our group as having an association with increased risk of RP, TGFB073 = TT, was marginally significant when included in the models containing XRCC_NCI and VEGF4039 ($p = 0.064$) or XRCC_NCI, VEGF4039 and TNF0629 ($p = 0.071$).

Conclusions: XRCC_NIH = WW and VEGF4039 = CT/TT were selected as significant adverse risk factors for RP in a Lyman model based on mean lung dose. TNF0629 = AA was also found to be a significant adverse risk factor, although there were only 4 patients with this genotype (3 of whom had severe RP). We are currently working on validating these findings in an independent cohort.

Author Disclosure: Z. Liao, None; Q. Wei, None; M.K. Martel, None; D. Gomez, None; Z. Liu, None; X. Guan, None; Y. Zhuang, None; C. Lu, None; R. Komaki, None; S.L. Tucker, None.

1132 The Value of Single Nucleotide Polymorphisms in TGFβ1, TPA and ACE in Survival Prediction in Patients with Non-small Cell Lung Cancer

C. Xie[1,2], S. Yuan[1,3], V. L. Ellingrod[4], J. A. Hayman[1], D. Arenberg[5], J. Curtis[5], N. Ramath[5], G. P. Kalemkerian[5], J. Wang[1], F. Kong[1]

[1]Department of Radiation Oncology, University of Michigan, Ann Arbor, MI, [2]The First Hospital of Wenzhou Medical College, Wenzhou, China, [3]Shandong Cancer Hospital and Institute, Jinan, China, [4]College of Pharmacy, University of Michigan, Ann Arbor, MI, [5]Department of Internal Medicine, University of Michigan, Ann Arbor, MI

Purpose/Objective(s): Single nucleotide polymorphisms (SNPs) of transforming growth factor belta1 (TGFβ1) are known to be associated with the risk of radiation induced lung toxicities. Tissue plasminogen activator (TPA), and angiotensin-converting enzyme (ACE) are also related to radiation damage. We hypothesized that single nucleotide polymorphisms (SNPs) of the functional regions of these genes may also be associated with survival in patients with non-small cell lung cancer (NSCLC).

Materials/Methods: Using 80 available genomic DNA samples from blood buffy coats of patients with NSCLC treated with definitive radiochemotherapy in a prospective study, we genotyped 3 SNPs of each gene (TGFβ1 gene, CC, CT and TT; TPA, CC,

JJCO Japanese Journal of Clinical Oncology

Jpn J Clin Oncol 2010;40(9)846–854
doi:10.1093/jjco/hyq134
Advance Access Publication 29 July 2010

Stereotactic Body Radiation Therapy for Lung Cancer: Achievements and Perspectives

Masahiro Hiraoka*, Yukinori Matsuo and Kenji Takayama

Department of Radiation Oncology and Image-applied Therapy, Kyoto University Graduate School of Medicine, Sakyoku, Kyoto, Japan

*For reprints and all correspondence: Masahiro Hiraoka, E-mail: hiraok@kuhp.kyoto-u.ac.jp

Received April 25, 2010; accepted June 21, 2010

Stereotactic body radiation therapy is a new treatment modality where narrow beams from several directions focus on the target while sparing the adjacent normal tissues with high accuracy. This technique basically derived from that of radiosurgery for intracranial lesions allows us to deliver high dose to the target leading to high control of the tumor without causing significant cytotoxicities associated with the treatment. Early-stage non-small cell lung cancers are regarded as most appropriate malignancies for this modality and accordingly have most intensively been investigated. With many encouraging outcomes in retrospective studies, several prospective clinical trials have been started world-wide. Japan Clinical Oncology Group protocol 0403 is a phase II trial of stereotactic body radiation therapy for T1N0M0 non-small cell lung cancer including both inoperable and operable patients. The results for operable patients are to be disclosed this year after 3 years of follow-up. It is highly probable that stereotactic body radiation therapy can be a standard treatment modality for inoperable patients for early-stage non-small cell lung cancer. The role of stereotactic body radiation therapy for operable patients is expected to be clarified by the outcomes of coming clinical trials. Tremendous advance in stereotactic body radiation therapy is expected when four-dimensional radiation therapy coping with tumor movement is realized. Among several approaches, tumor tracking appears most ideal. The new image-guided radiotherapy system which has the capability of tumor tracking has been developed in Japan.

Key words: stereotactic body radiation therapy – non-small cell lung cancer – four-dimensional radiation therapy – tumor tracking

INTRODUCTION

Radiation therapy (RT) is recognized as one of three major treatment modalities in the management of cancer. The ratio of newly diagnosed cancer patients treated by RT is around 60% in developed countries. The only exception is Japan where only 25% of patients receive RT as of 2004. The ratio has increased by 10% in the last decade, and it is estimated that it will be up to 40% in 2015 (1). The rapid increase in elderly patients, who are not amenable to surgical treatment, and innovations of RT in both physical and biological aspects to meet the demands of patients explain this increased use of RT.

The goal of RT is to accomplish the improvement of survival and also the improvement of quality of life in cancer patients. There are two limiting factors to achieve this goal in current RT. One is insufficient biological effects of radiotherapy, and the other is unsatisfactory dose localization techniques. To overcome these problems, several strategies have been investigated, which are divided into two approaches, one is a biological approach and the other is a physical one. The biological approach includes combination of anti-cancer drugs with RT (chemoradiotherapy), modification of fractionation regimen, use of radiosensitizers or radioprotectors, use of hyperthermia and heavy particle therapy. As regards the physical approach, which allows us to irradiate the target as most physically localized as possible, there are intraoperative RT, brachytherapy, conformal radiotherapy, three-dimensional conformal RT (3DCRT), stereotactic irradiation (STI), intensity-modulated RT (IMRT) and proton or heavy particle therapy.

Among those approaches, chemoradiotherapy, STI, IMRT and proton or heavy particle therapy have been applied intensively in clinics as advanced RT modalities.

STI started with intracranial lesions in 1960s. The great success of this innovative treatment, in terms of the technologies used, quality assurance and quality control and clinical outcomes indicating high local control rate with minimal toxicities has induced much interest in the application of this treatment for extracranial regions (2,3). The technologies and methods have been improved greatly in the last decade, and now it is used in clinics as an effective treatment for tumors including early-stage non-small cell lung cancer (NSCLC), liver tumor and so on. STI for extracranial lesions is usually named as stereotactic body RT (SBRT). Radiation oncologists in Japan have contributed greatly to the development of this innovative treatment modality, and furthermore are leading the next generation of SBRT, that is four-dimensional SBRT.

In this 40th anniversary issue of Japanese Journal of Clinical Oncology, achievements and future perspectives of SBRT will be reviewed focusing on studies in Japan.

CONCEPT AND HISTORY

STI was originally developed by Leksell (4) for intracranial lesions. The concept of this new treatment technology is that narrow beams from several directions focus on the target while sparing the adjacent normal tissues with high accuracy. This technique allows us to deliver high dose to the target leading to high control of the tumor without causing significant cytotoxicities associated with the treatment. The Gamma Knife had been invented for this purpose and installed at Karolinska Hospital in 1968. Following the great success of the Gamma Knife, linear accelerator (LINAC)-based STI has been developed. It is advantageous over the Gamma Knife in that fractionated irradiation is feasible. With the use of fractionated STI, function preservation rate (like hearing capability) is improved and relatively larger tumors can be treated (5).

SBRT is an applied form of STI. It has taken a few decades for STI to be applied for extracranial lesions since the Gamma Knife had been invented. There were several issues to be resolved before it could be utilized for extracranial organs: computed tomography (CT) which can visualize and localize lesions precisely, a treatment planning system for 3D dose calculation and a fixation device for the body. Lax et al. (6) developed the first stereotactic body frame with vacuum pillow stabilization for SBRT in 1994. Blomgren et al. (2) published the first report on SBRT using the stereotactic body frame in 1995. Forty-two tumors in the lung and liver of 31 patients were treated with SBRT. The local control rate was 80%. In Japan, Uematsu et al. (3) developed a frameless system (FOCAL unit) that consisted of a LINAC, an X-ray simulator, CT and a table. They treated 66 lung tumors in 45 patients using this system. Local progression was observed only in 2 of the 66 tumors (3%). Several researchers studied SBRT for lung tumors after these reports, and their results were also promising. These promising results encouraged multi-institutional oncology groups to conduct trials of SBRT for the lung. The Radiation Therapy Oncology Group (RTOG) and Japan Clinical Oncology Group (JCOG) started the RTOG 0236 protocol and JCOG 0403 protocol, respectively.

Since SBRT was covered by the governmental health insurance in Japan in 2004, the number of patients treated with SBRT is increasing. SBRT was performed in 2104 cases with lung cancer at 53 institutions in Japan as of November 2004 (7).

RATIONALES AND INDICATIONS

The use of a high dose per fraction with small fraction number (hypofractionation) for a small tumor is the basis of SBRT. This approach is a double-edged sword. This scheme provides much higher effects on the tumor compared with conventionally fractionated RT, while much worse influence on normal tissues. This is because irradiation with high dose per fraction has been shown to produce more toxicities in a late phase. Prerequisites for SBRT are (i) the lesion is clearly visualized; (ii) the target is precisely localized; (iii) no serial organs are adjacent to the lesion and (iv) tumor size is relatively small. Considering these conditions, the lung and the liver are most suitable for SBRT. Recently, SBRT has been investigated clinically for cancers in the pancreas (8), the prostate (9), paraspinal areas (10) and so on.

Lung cancer is the leading cause of cancer-related death in Japan (11). Approximately 65 000 patients died of lung cancer in 2007 in Japan. For the management of stage I NSCLC, surgical resection is the standard treatment, and lobectomy is generally accepted as the optimal surgical procedure. Survival outcomes of surgical treatment have recently been reported by the Japanese Joint Committee of Lung Cancer Registry (12). According to these data, the overall survival of patients in clinical stage IA is 77.3% at 5 years, and that of patients in clinical stage IB is 59.8% at 5 years.

What about RT alone for stage I NSCLC? As is known, RT has been used primarily for those patients who are not considered to be surgical candidates; that is, those who refuse surgical intervention, and those who are medically inoperable. The reported 5-year survival rate is around 6–32%, and is not satisfactory (13). SBRT is expected to improve the outcomes for these patients.

TECHNIQUES

Details on SBRT procedures for lung cancer in Kyoto University were described in the previous paper (14). The criteria for SBRT for lung tumors were one or two tumors in

the lung with size <5 cm in diameter. Two kinds of body frame, Stereotactic Body Frame (Elekta, Stockholm, Sweden) and BodyFIX (Medical Intelligence, Schwabmünchen, Germany), are used to attain accurate and precise patient positioning and immobilization. The former has built-in reference indicators which provide accurate determination of target coordinates. In our experience, daily setup errors with Stereotactic Body Frame were within 5 mm in 90, 100 and 93% of all verifications in the mediolateral, anteroposterior and craniocaudal directions, respectively (15). BodyFIX is composed of radiolucent materials that allow image guidance with X-ray.

X-ray fluoroscopy is performed to measure tumor movement before CT scan. When the tumor moves more than 8 mm in the craniocaudal direction, we use a small plate called a 'diaphragm control' which suppresses the movement of the diaphragm and reduces respiratory motion of the tumor. After fluoroscopy, the patient is transferred to a CT room. CT scan is performed under free-breathing with a slow scan technique which can visualize a major part of the trajectory of the tumor by scanning each slice for a time longer than the respiratory cycle, or a 4D-CT technique.

The internal target volume (ITV), which encompasses the whole trajectory of the tumor motion, is delineated on the scanned CT images. After contouring on CT, we compare the ITV on CT with the tumor motion, which was evaluated on fluoroscopy. If the delineated ITV is found to be insufficient to encompass respiratory motion, we extend the ITV. The planning target volume (PTV) is defined by adding a 5-mm margin of setup error to the ITV. The planning organ-at-risk volumes (PRVs) are defined for lung, spinal cord, esophagus, stomach, intestine, trachea, bronchus, pulmonary artery and other organs at risk (OARs). The margin between PRV and OAR is 5 mm, except for the spinal cord and lung. The PRV for the spinal cord is defined as a 3-mm margin with the spinal canal delineated on CT images. The PRV for the lung is the bilateral pulmonary parenchyma outside the PTV. Non-coplanar static beams (5–8 ports) with 6-megavolt (MV) X-rays are used. The margin between the PTV and the field edge is 5 mm, as a rule.

We prescribe a total dose of 48 Gy in four fractions at the isocenter for primary lung cancer with a diameter of 3 cm or less, and 56 Gy in 14-Gy fractions for primary tumor larger than 3 cm and metastatic lung cancer, respectively. Calculated biological effective doses (BEDs) are 105.6 and 134.4 Gy at the isocenter (under $\alpha/\beta = 10$ Gy), respectively.

CLINICAL OUTCOMES

Primary NSCLC

Table 1 summarizes reports on outcomes of SBRT for NSCLC. There are some variations in dose-fractionation and patient characteristics including operability. It is obvious that SBRT outcomes are much better than those of conventional radiotherapy persistently.

We recently reviewed 10-year experiences at Kyoto University to investigate the factors that influence clinical outcomes following SBRT for lung cancer (16). A total of 101 patients with histologically confirmed stage I NSCLC who underwent SBRT with 48 Gy in four fractions from September 1998 to December 2007 were examined. Multivariate analysis using the Cox proportional hazards model was used to find potential factors that affected clinical outcomes after SBRT. The factors evaluated were age, maximal diameter of tumor, overall treatment time, sex, performance status, operability and histology. The analysis has revealed that tumor diameter and sex were the most significant factors. Recursive partitioning analysis indicated a condition for good prognosis (class I) as follows: female or T1a (tumor diameter ≤20 mm). When the remaining male patients with T1b–2a (>20 mm) were defined as class II, 3-year rates of local progression, disease progression and overall survival were 6.8, 23.6 and 69.9% in class I, respectively, whereas these values were 19.9, 58.3 and 47.1% in class II. The differences between the classes were statistically significant.

There are two large series of multi-institutional studies that retrospectively surveyed clinical outcomes of SBRT for NSCLC. Onishi et al. (17) reviewed 257 patients who

Table 1. A summary of outcomes after SBRT for primary lung cancer

Author	Year	No. of cases	T-stage (T1:T2)	Dose	3y LC	3y OS	MST (mo)
Nyman et al. (39)	2006	45	18:27	45 Gy/3 fr.	80%	55%	39
Hoyer et al. (40)	2006	40	22:18	45 Gy/3 fr.	85% (2y)	48% (2y)	NA
Koto et al. (41)	2007	31	19:12	45 Gy/3 fr. or 60 Gy/8 fr.	77.9% (T1)	71.7%	NA
Fakiris et al. (42)	2009	70	34:36	60 or 66 Gy/3 fr.	88.1%	42.7%	32.4
Ricardi et al. (43)	2009	62	43:19	45 Gy/3 fr.	87.8%	57.1%	NA
Kopek et al. (44)	2009	88	51:36	45 or 67.5 Gy/3 fr.	89%	36%	21.8
Matsuo et al. (16)	2010	101	73:28	48 Gy/4 fr.	86.8%	58.6%	48.8

SBRT, stereotactic body radiation therapy; LC, local control; OS, overall survival; MST, median survival time.

underwent SBRT for stage I NSCLC during 1995–2004 at 14 institutions in Japan. Local progression was observed in 14.0% of patients. The overall 3- and 5-year survival rates were 56.8 and 47.2%, respectively. The local recurrence rates were 8.4% in patients who received a BED of 100 Gy or more at the isocenter, and 42.9% in patients receiving a BED <100 Gy. This difference was statistically highly significant ($P < 0.001$). Baumann et al. (18) retrospectively reviewed results of SBRT for 138 patients with medically inoperable stage I NSCLC treated during 1996–2003 at five centers in Sweden and Denmark. Local failure was observed in 12% of patients. The overall 3- and 5-year survival rates were 52 and 26%, respectively. Local failure was associated with tumor size, target definition and central or pleura proximity. There was a significant advantage in survival for the group receiving a dose above 55.6 Gy in equivalent dose in 2 Gy fractions (EQD2). This report indicates that 55.6 Gy in EQD2 at the PTV periphery corresponds to BED of 100 Gy at the isocenter as is shown in the Onishi's study.

Two multi-institutional prospective trials of SBRT for primary lung cancer have been reported so far. One is a phase II trial for inoperable stage I NSCLC which was undertaken at seven centers in Sweden, Norway and Denmark (19). The prescription dose was 15 Gy with a total dose of 45 Gy at the 67% isodose of the PTV. The 3-year local control rate and overall the survival rate were 92 and 60%, respectively, at a median follow-up of 35 months. Another trial is RTOG protocol 0236 (20). A total dose of 60 Gy was delivered in three fractions to cover 95% of the PTV. Three-year estimates of disease-free and overall survival were 48.3 and 55.8%, respectively.

JCOG protocol 0403 is a phase II trial of SBRT for T1N0M0 lung cancer including both inoperable and operable patients. Patient accrual for operable cases and their 3-year follow-up has already finished in February 2010, and the outcomes are to be disclosed in 2010. This is the first prospective trial for operable T1N0M0 lung cancer (21).

Metastatic Lung Cancer

There are several reports on SBRT for metastatic lung cancer (Table 2). Up to two lesions were simultaneously treated in most of these reports, except for that by Okunieff (up to five lesions). The local control rate was around 80% and the overall survival rate was more than 30% at 2 years. These outcomes seem comparable to those by surgical metastatectomy (22).

Rusthoven et al. (23) reported a multi-institutional phase I/II trial of SBRT for metastatic lung tumor. Actuarial local control rate at 1 and 2 years after SBRT was 100 and 96%, respectively, at a median follow-up of 15.4 months. Median survival was 19 months, and overall survival rate at 2 years was 39%.

Complications

Onishi et al. (17) reported that pulmonary complications above grade 2 were observed in 5.4%, grade 3 esophagitis in 0.8% and grade 3–4 dermatitis in 1.2% in the retrospective study of 257 SBRT patients. In Baumann's retrospective study, grade 3–4 toxicity was observed in 10.1% (18).

One of the most informative reports on toxicities associated with SBRT for the lung cancer is the article published in 2006 by Timmerman et al. (24). They reported that grade 5 toxicity was observed in 6 patients (8.6%), and grade 3–4 was in the 8 patients (11.4%) of 70 patients who underwent SBRT for NSCLC with a prescription dose of 60–66 Gy in three fractions. Such severe toxicities were related with tumor location. Patients treated for tumors in the peripheral lung demonstrated a 2-year freedom from severe toxicity in 83% compared with 54% for patients with central tumors. On the basis of this study, central tumor was excluded from the RTOG trial 0236. Protocol-related grade 3 and 4 adverse events in the RTOG 0236 were reported in 12.7 and 3.6%, respectively (20).

PERSPECTIVES OF CLINICAL ISSUES

SBRT for Centrally Located Tumors

Relatively, few data have been available for centrally located tumors. Timmerman et al. (24) demonstrated that a total dose of 60–66 Gy in three fractions caused severe toxicities in 40% for centrally located tumors in the lung. The dose to the organs in the mediastinum should be low enough in those tumors. One possible approach to a central tumor is the use of a mild hypofractionation regimen with a smaller

Table 2. A summary of outcomes after SBRT for metastatic lung tumor

Author	Year	No. of cases/lesions	Dose	LC (%)	OS (%)
Onimaru et al. (26)	2003	20/32	48–60 Gy/8 fr.	93.8	48.8
Wulf et al. (45)	2004	41/51	26 Gy/1 fr. or 30–37.5 Gy/3 fr.	80	33
Okunieff et al. (46)	2006	50/125	50–55 Gy/10–11 fr.	83	38
Hof et al. (47)	2007	61/71	12–30 Gy/1 fr.	73.7	65.1
Norihisa et al. (48)	2008	34/43	48–60 Gy/4–5 fr.	90.0	84.3
Kim et al. (49)	2009	13/18	39–51 Gy/3 fr.	52.7	75.5

fractional dose. Lagerwaard et al. (25) used three fractionation schemes depending on T-stage and normal tissue toxicity; three fractions of 20 Gy (for T1 tumors), five fractions of 12 Gy (for T1 tumors showing broad contact with the thoracic wall, or T2 tumors) or eight fractions of 7.5 Gy (for tumors adjacent to the heart, hilus or mediastinum). They reported that this risk-adapted SBRT was well tolerated and severe late toxicity was observed in <3% of patients. Eight fractions of 7.5 Gy may be a reasonable approach for most central tumors. There is a case report that a lower dose of 48 Gy in eight fractions caused a grade 5 esophageal ulcer (26). Further studies are needed to determine an optimal dose and fractionation for centrally located tumors.

SBRT for Operable Patients

One of the biggest questions to be answered is whether SBRT can be an alternative to surgical treatment. Several results suggest the potential use of SBRT for those patients. JCOG0403 to be open this year will answer this question since it is the first prospective trial dealing with operable patients. If the results appear almost equivalent to those of surgery, a phase III trial which randomizes lobectomy with SBRT is obviously warranted.

In conclusion, technologies of SBRT have been almost established in the last decade. Clinical efficacy and safety of SBRT for lung cancers are being evaluated favorably by clinical studies. SBRT is less invasive than surgery, and it can play an important role for operable patients with early-stage NSCLC who refuse surgery due to the invasiveness, especially for elderly patients. For inoperable patients, SBRT is considered as a standard treatment with curative intent.

PERSPECTIVES OF INNOVATIONS FROM 3DRT TO 4DRT

Three-dimensional conformal irradiation techniques have improved the dose distributions greatly. It enabled the delivery of high-dose irradiation to the target while minimizing the dose to the surrounding normal tissues. The most advanced treatment of this 3DCRT is STI and IMRT, and many patients with cancer enjoy the benefits of this innovative treatment.

Tremendous advance in sophisticated RT is expected when 3DRT is moved up to 4DRT (four-dimensional RT). Almost all tumors in the body are never static. A tumor in the intra-thoracic and upper-abdominal regions may move 1–3 cm with respiration (27,28). If sufficiently large safety margins are setup to encompass large tumor motions, a large amount of normal tissues have to be irradiated, which obviously increases the risk of radiation-induced cytotoxicities. Several approaches to compete with tumor motions have been clinically attempted, including respiratory inhibition with abdominal compression (15), breath-holding (29,30), respiratory gating (31–33) and tumor tracking. The 4DRT is generally defined in that information on the target position is tracked directly or indirectly in real-time during the treatment session, and the treatment beams are adaptively delivered in accordance with the motion information. Realization of this 4DRT obviously will open a new era of external RT. It will dramatically improve the tumor conformality, and accordingly SBRT and IMRT will be applied to larger tumors and malignancies in various sites for which 3DRT has contributed little.

HISTORY OF THE 4DRT

Japan has contributed much to the development of the 4DRT. In the late 1980s and early 1990s, respiratory gating in RT was first studied by Ohara et al. (31) to apply proton therapy mostly for liver tumors. They used a pressure sensor for the abdominal wall as a respiratory signal. This method was followed by Minohara et al. (32) in gated heavy-ion beam treatment. In the USA, in the mid 1990s, Kubo and Hill (33) investigated different external respiratory signals to monitor respiratory motion. Currently, gated radiotherapy using an external respiratory signal has being clinically implemented using commercially available systems. One of the problems of this method is low duty cycle (typically 30–50%). Since the beam is not continuously delivered, gating procedures take longer treatment time than non-gating procedures. Another problem is that the time-dependant target position might not match the respiration monitoring, and position accuracy is not always guaranteed.

To solve the latter problem, Hokkaido University and Mitsubishi Electronics Co. Ltd developed a new approach in the late 1990s, named 'real-time tumor-tracking radiotherapy (RTRT) system.' It consists of four diagnostic X-ray fluoroscopy units located in a radiation treatment room. Two units of the four are used to track 2-mm gold fiducial markers inserted in or near the tumor using image-guided implantation, and the 3D position of the each fiducial can be calculated every 0.03 s in real-time. The LINAC is gated to irradiate the tumor when each fiducial is within an acceptable range of the desired position (34,35). This system realized real-time tracking radiotherapy, and enabled us to know the details of tumor motion by respiration, which have not been evaluated. However, since the beam delivery method is categorized as gated radiotherapy, the problem of treatment time prolongation has still remained. In addition, this system requires implantation of gold fiducial markers. Unfortunately, the system has not been distributed in the world market, and finally discontinued from production.

An attractive and ideal approach to compete with tumor movement is dynamic-tracking irradiation in which the beam is continuously delivered focusing on the tumor. It is advantageous in that beam delivery is highly efficient and the procedure is totally non-invasive. Figure 1 summarized differences between a conventional method with wide margin, respiratory gating and dynamic-tracking irradiation.

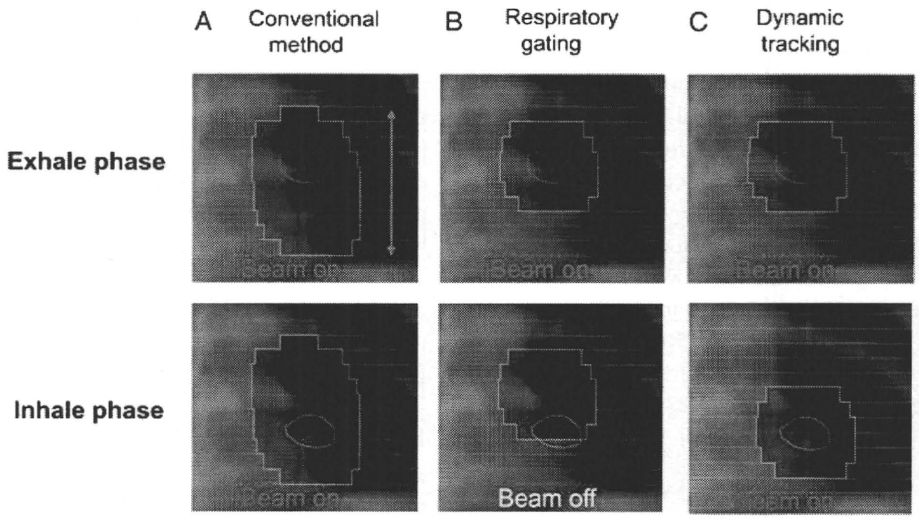

Figure 1. From 3DRT to 4DRT. (A) Conventional method: Wide margin is needed to include respiratory motion. It causes excess irradiation to the normal tissue. (B) Respiratory gating: Beam delivery is gated. Treatment time is prolonged. (C) Dynamic tracking: Beam tracks the target. It allows continuously irradiation with a small field.

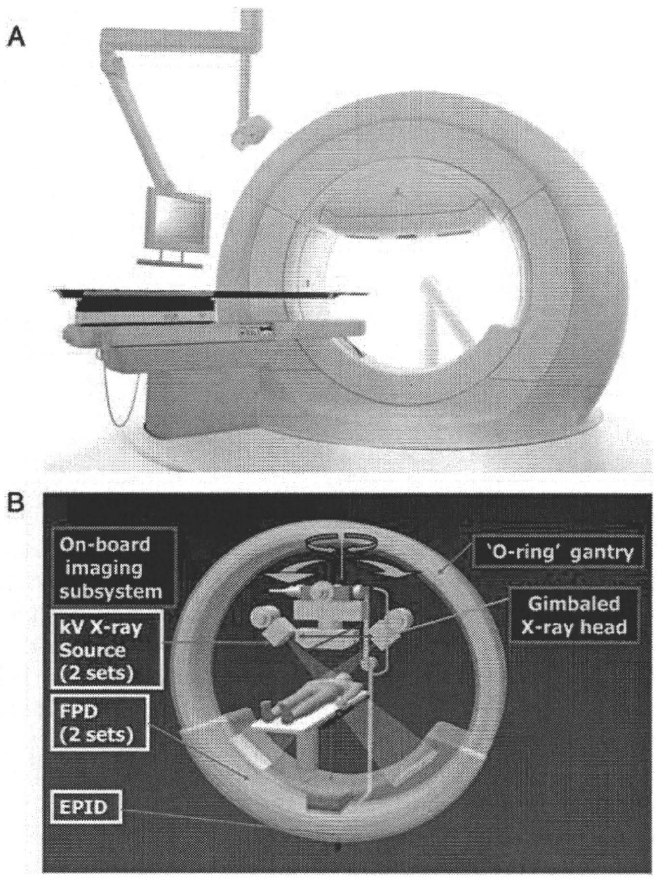

Figure 2. An innovative image-guided radiotherapy (IGRT) system 'MHI-TM2000'. (A) Overview of the machine. (B) Configuration of the system. Abbreviations: FPD, flat panel detector; EPID, electronic portal imaging device.

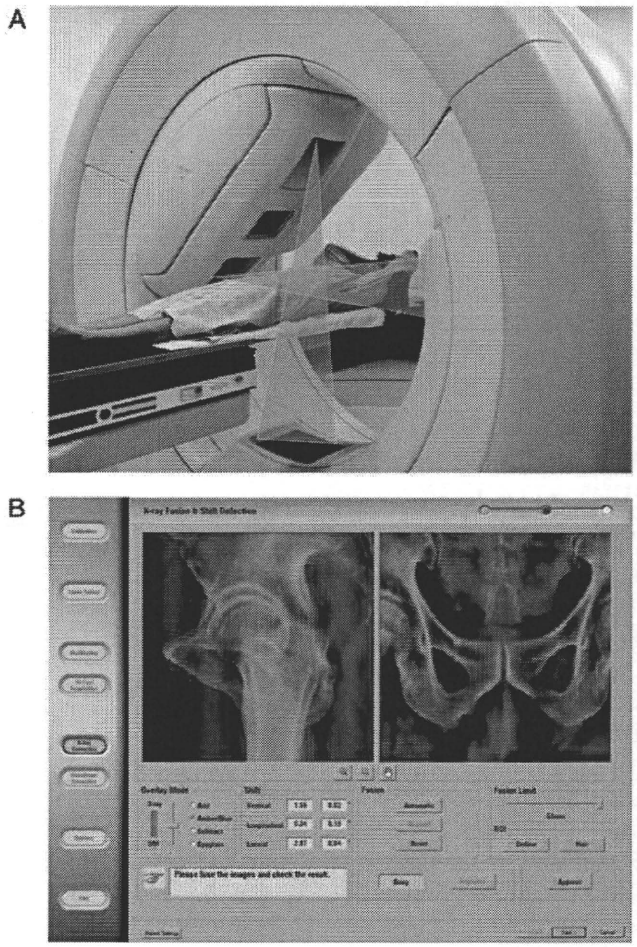

Figure 3. Image-guided setup using simultaneously obtained orthogonal radiographs. (A) Dual kilovoltage (kV) X-ray imaging subsystem consisting of two sets of a kV X-ray tube and an FPD provides simultaneous orthogonal radiographs. (B) The obtained radiographs are automatically registered to the digitally reconstructed radiographs (DRR) for image-guided setup based on bone structures.

Kyoto University, Institute of Biomedical Research and Innovation (IBRI) and Mitsubishi Heavy Industries, Ltd have started collaboration in 2000 to develop an innovative

image-guided radiotherapy (IGRT) system which has the capability of dynamic tumor tracking using a novel gimbaled X-ray head and a dual real-time X-ray monitoring system (36–38). The first clinical version of the IGRT system has been approved in FDA in August 2007 and PMDA in January 2008 as 'MHI-TM2000.' Its clinical application started in May 2008 at IBRI, and five machines are working or are under construction in Japan and in Belgium as of March 2010.

DYNAMIC TUMOR-TRACKING IRRADIATION BY MHI-TM2000

The configuration of MHI-TM2000 is shown in Fig. 2. The system is designed to efficiently implement genuine high-precision radiotherapy. A rigid ring gantry supports both the beam delivery system and on-board imaging system. An on-board dual kilovoltage X-ray imaging system provides orthogonal radiographs or cone-beam CT (CBCT) for an image-guided setup. The setup error is automatically calculated by the image registration software shown in Fig. 3, and a patient support couch can automatically correct the error not only in translational shift but also rotational movement. The beam delivery system consists of an originally developed C-band compact LINAC which produces 6-MV photon beam, and a multi-leaf collimator (MLC) which produces conformal beams for 3DCRT or intensity-modified beams for IMRT. These components above are highly integrated to implement a fast and accurate image-guided setup and precise beam delivery. Those capabilities are being investigated clinically for 150 patients treated at IBRI.

The X-ray head with the LINAC and the MLC is mounted on a gimbals mechanism. As illustrated in Fig. 4, the gimbals mechanism has two rotational axes, and an active control of rotations along these axes allows the treatment beam to swing toward a designated position around the isocenter. Each rotation (pan and tilt motion) ranges up to $+/-2.4°$, which means that the MV beam can swing in the range of up to $+/-4.2$ cm from the isocenter. This beam swing function can be used to achieve high accuracy of the beam delivery to the mechanical isocenter by active compensation for any mechanical distortion in the static mode. A star-shot irradiation test demonstrated its high-beam positioning accuracy <0.1 mm. In the dynamic mode, this function enables the MV beams to track a target in real-time while continuously being delivered. This dynamic-tracking irradiation method named 'gimbaled tracking' has three advantages. First, one-degree-ordered small-angle rotations of the gimbals provide quick and accurate beam adaptation to designated positions of a mobile target. Secondly, the mechanism is relatively simple and thus minimizes mechanical load. Finally, the treatment system is safer than systems involving a robotic arm because the moving unit is covered so as not to touch a patient.

In terms of real-time imaging, the system can use orthogonal serial radiographs scanned with the gantry-mounted kilovoltage X-ray imaging system. This technique is capable of directly tracking tumors based on the density difference between the tumor and normal lung tissue, provided that the tumor is well defined with a high-contrast edge. Several variations for real-time tracking would be possible in a clinical setting, such as direct tracking, external surrogates and internal surrogates including fiducial markers, diaphragms and so on.

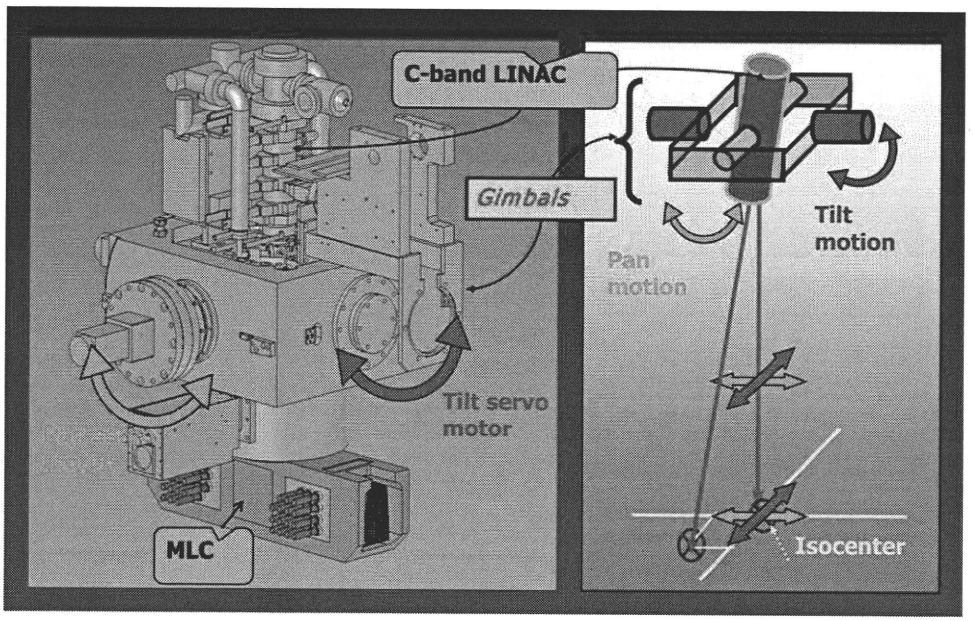

Figure 4. Gimbaled X-ray head. X-ray head with a LINAC and an MLC is mounted on a gimbals mechanism. Rotations along the two orthogonal gimbals (pan and tilt rotations) up to $+/-2.4°$ allow the therapeutic beam swing toward a designated position in the range of up to $+/-4.2$ cm from the isocenter. Abbreviations: LINAC, linear accelerator; MLC, multi-leaf collimator.

The validation tests using a computer-controlled three-dimensionally movable phantom have shown that the gimbals tracking system significantly reduced motion blurring effects in the dose distribution compared with the non-tracking state, and produced a dose profile slope similar to the profile that is obtained when the phantom was stationary (<1 mm) (37,38). Currently, the gimbals tracking irradiation function is not installed in a commercially available version. Mitsubishi Heavy Industries is developing a clinically applicable system in collaboration with Kyoto University and IBRI.

CONCLUSIONS

SBRT is an innovative treatment modality for early-stage NSCLC. It is considered to be a standard treatment option for inoperable patients. The role of SBRT for early-stage NSCLC should be clarified by the coming clinical trials.

Realization of four-dimensional RT coping with tumor movement obviously causes dramatic advancement of SBRT. The new IGRT system which has the capability of tumor tracking has been developed in Japan, and is expected to be applied in clinics.

Funding

This work was partially supported by a Grant-in-Aid for Scientific Research (S) from Japan Society for the Promotion of Science (No. 20229009); and a grant for Practical Application of Next-generation Strategic Technology Commissioned by New Energy and Industrial Technology Development Organization of Japan (No. 0901002-2006).

Conflict of interest statement

Masahiro Hiraoka and Kenji Takayama have a consultancy agreement with Mitsubishi Heavy Industries.

References

1. Teshima T, Numasaki H, Shibuya H, Nishio M, Ikeda H, Ito H, et al. Japanese structure survey of radiation oncology in 2005 based on institutional stratification of patterns of care study. *Int J Radiat Oncol Biol Phys* 2008;72: 144–52.
2. Blomgren H, Lax I, Näslund I, Svanström R. Stereotactic high dose fraction radiation therapy of extracranial tumors using an accelerator. Clinical experience of the first thirty-one patients. *Acta Oncol* 1995;34:861–70.
3. Uematsu M, Shioda A, Tahara K, Fukui T, Yamamoto F, Tsumatori G, et al. Focal, high dose, and fractionated modified stereotactic radiation therapy for lung carcinoma patients: a preliminary experience. *Cancer* 1998;82:1062–70.
4. Leksell L. Stereotactic radiosurgery. *J Neurol Neurosurg Psychiatry* 1983;46:797–803.
5. Andrews DW, Suarez O, Goldman HW, Downes MB, Bednarz G, Corn BW, et al. Stereotactic radiosurgery and fractionated stereotactic radiotherapy for the treatment of acoustic schwannomas: comparative observations of 125 patients treated at one institution. *Int J Radiat Oncol Biol Phys* 2001;50:1265–78.
6. Lax I, Blomgren H, Näslund I, Svanström R. Stereotactic radiotherapy of malignancies in the abdomen. Methodological aspects. *Acta Oncol* 1994;33:677–83.
7. Nagata Y, Hiraoka M, Mizowaki T, Narita Y, Matsuo Y, Norihisa Y, et al. Survey of stereotactic body radiation therapy in Japan by the Japan 3-D conformal external beam radiotherapy group. *Int J Radiat Oncol Biol Phys* 2009;75:343–7.
8. Chang DT, Schellenberg D, Shen J, Kim J, Goodman KA, Fisher GA, et al. Stereotactic radiotherapy for unresectable adenocarcinoma of the pancreas. *Cancer* 2009;115: 665–72.
9. King CR, Brooks JD, Gill H, Pawlicki T, Cotrutz C, Presti JC. Stereotactic body radiotherapy for localized prostate cancer: interim results of a prospective phase II clinical trial. *Int J Radiat Oncol Biol Phys* 2009;73:1043–8.
10. Chang EL, Shiu AS, Mendel E, Mathews LA, Mahajan A, Allen PK, et al. Phase I/II study of stereotactic body radiotherapy for spinal metastasis and its pattern of failure. *J Neurosurg Spine* 2007;7:151–60.
11. Foundation for Promotion of Cancer Research. Cancer Statistics in Japan. 2009; http://ganjoho.ncc.go.jp/public/statistics/backnumber/2009_en.html.
12. Asamura H, Goya T, Koshiishi Y, Sohara Y, Eguchi K, Mori M, et al. A Japanese Lung Cancer Registry study: prognosis of 13,010 resected lung cancers. *J Thorac Oncol* 2008;3:46–52.
13. Sibley GS. Radiotherapy for patients with medically inoperable Stage I nonsmall cell lung carcinoma: smaller volumes and higher doses—a review. *Cancer* 1998;82:433–8.
14. Takayama K, Nagata Y, Negoro Y, Mizowaki T, Sakamoto T, Sakamoto M, et al. Treatment planning of stereotactic radiotherapy for solitary lung tumor. *Int J Radiat Oncol Biol Phys* 2005;61:1565–71.
15. Negoro Y, Nagata Y, Aoki T, Mizowaki T, Araki N, Takayama K, et al. The effectiveness of an immobilization device in conformal radiotherapy for lung tumor: reduction of respiratory tumor movement and evaluation of the daily setup accuracy. *Int J Radiat Oncol Biol Phys* 2001;50:889–98.
16. Matsuo Y, Shibuya K, Nagata Y, Takayama K, Norihisa Y, Takashi M, et al. Prognostic factors in stereotactic body radiation therapy for non-small-cell lung cancer. *Int J Radiat Oncol Biol Phys* 2010; doi: 10.1016/j.ijrobp.2009.12.022.
17. Onishi H, Shirato H, Nagata Y, Hiraoka M, Fujino M, Gomi K, et al. Hypofractionated stereotactic radiotherapy (HypoFXSRT) for stage I non-small cell lung cancer: updated results of 257 patients in a Japanese multi-institutional study. *J Thorac Oncol* 2007;2(7 Suppl 3):S94–S100.
18. Baumann P, Nyman J, Lax I, Friesland S, Hoyer M, Ericsson SR, et al. Factors important for efficacy of stereotactic body radiotherapy of medically inoperable stage I lung cancer. A retrospective analysis of patients treated in the Nordic countries. *Acta Oncol* 2006;45:787–95.
19. Baumann P, Nyman J, Hoyer M, Wennberg B, Gagliardi G, Lax I, et al. Outcome in a prospective phase II trial of medically inoperable stage I non-small-cell lung cancer patients treated with stereotactic body radiotherapy. *J Clin Oncol* 2009;27:3290–6.
20. Timmerman R, Paulus R, Galvin J, Michalski J, Straube W, Bradley J, et al. Stereotactic body radiation therapy for inoperable early stage lung cancer. *JAMA* 2010;303: 1070–6.
21. Hiraoka M, Ishikura S. A Japan clinical oncology group trial for stereotactic body radiation therapy of non-small cell lung cancer. *J Thorac Oncol* 2007;2(7 Suppl 3):S115–7.
22. The International Registry of Lung Metastases Writing Committee. Long-term results of lung metastasectomy: prognostic analyses based on 5206 cases. *J Thorac Cardiovasc Surg* 1997;113:37–49.
23. Rusthoven KE, Kavanagh BD, Burri SH, Chen C, Cardenes H, Chidel MA, et al. Multi-institutional phase I/II trial of stereotactic body radiation therapy for lung metastases. *J Clin Oncol* 2009;27:1579–84.
24. Timmerman R, McGarry R, Yiannoutsos C, Papiez L, Tudor K, DeLuca J, et al. Excessive toxicity when treating central tumors in a phase II study of stereotactic body radiation therapy for medically inoperable early-stage lung cancer. *J Clin Oncol* 2006;24:4833–9.
25. Lagerwaard FJ, Haasbeek CJ, Smit EF, Slotman BJ, Senan S. Outcomes of risk-adapted fractionated stereotactic radiotherapy for stage I non-small-cell lung cancer. *Int J Radiat Oncol Biol Phys* 2008;70:685–92.

26. Onimaru R, Shirato H, Shimizu S, Kitamura K, Xu B, Fukumoto SI, et al. Tolerance of organs at risk in small-volume, hypofractionated, image-guided radiotherapy for primary and metastatic lung cancers. *Int J Radiat Oncol Biol Phys* 2003;56:126–35.
27. Keall PJ, Mageras GS, Balter JM, Emery RS, Forster KM, Jiang SB, et al. The management of respiratory motion in radiation oncology report of AAPM Task Group 76. *Med Phys* 2006;33:3874–900.
28. Shirato H, Suzuki K, Sharp GC, Fujita K, Onimaru R, Fujino M, et al. Speed and amplitude of lung tumor motion precisely detected in four-dimensional setup and in real-time tumor-tracking radiotherapy. *Int J Radiat Oncol Biol Phys* 2006;64:1229–36.
29. Onishi H, Kuriyama K, Komiyama T, Tanaka S, Sano N, Aikawa Y, et al. A new irradiation system for lung cancer combining linear accelerator, computed tomography, patient self-breath-holding, and patient-directed beam-control without respiratory monitoring devices. *Int J Radiat Oncol Biol Phys* 2003;56:14–20.
30. Wong JW, Sharpe MB, Jaffray DA, Kini VR, Robertson JM, Stromberg JS, et al. The use of active breathing control (ABC) to reduce margin for breathing motion. *Int J Radiat Oncol Biol Phys* 1999;44:911–9.
31. Ohara K, Okumura T, Akisada M, Inada T, Mori T, Yokota H, et al. Irradiation synchronized with respiration gate. *Int J Radiat Oncol Biol Phys* 1989;17:853–7.
32. Minohara S, Kanai T, Endo M, Noda K, Kanazawa M. Respiratory gated irradiation system for heavy-ion radiotherapy. *Int J Radiat Oncol Biol Phys* 2000;47:1097–103.
33. Kubo HD, Hill BC. Respiration gated radiotherapy treatment: a technical study. *Phys Med Biol* 1996;41:83–91.
34. Shirato H, Shimizu S, Shimizu T, Nishioka T, Miyasaka K. Real-time tumour-tracking radiotherapy. *Lancet* 1999;353:1331–2.
35. Shirato H, Shimizu S, Kitamura K, Nishioka T, Kagei K, Hashimoto S, et al. Four-dimensional treatment planning and fluoroscopic real-time tumor tracking radiotherapy for moving tumor. *Int J Radiat Oncol Biol Phys* 2000;48:435–42.
36. Kamino Y, Takayama K, Kokubo M, Narita Y, Hirai E, Kawawda N, et al. Development of a four-dimensional image-guided radiotherapy system with a gimbaled X-ray head. *Int J Radiat Oncol Biol Phys* 2006;66:271–8.
37. Nakayama H, Mizowaki T, Narita Y, Kawada N, Takahashi K, Mihara K, et al. Development of a three-dimensionally movable phantom system for dosimetric verifications. *Med Phys* 2008;35:1643–50.
38. Takayama K, Mizowaki T, Kokubo M, Kawada N, Nakayama H, Narita Y, et al. Initial validations for pursuing irradiation using a gimbals tracking system. *Radiother Oncol* 2009;93:45–9.
39. Nyman J, Johansson KA, Hultén U. Stereotactic hypofractionated radiotherapy for stage I non-small cell lung cancer—mature results for medically inoperable patients. *Lung Cancer* 2006;51:97–103.
40. Hoyer M, Roed H, Hansen AT, Ohlhuis L, Petersen J, Nellemann H, et al. Prospective study on stereotactic radiotherapy of limited-stage non-small-cell lung cancer. *Int J Radiat Oncol Biol Phys* 2006;66(4 Suppl 1):S128–35.
41. Koto M, Takai Y, Ogawa Y, Matsushita H, Takeda K, Takahashi C, et al. A phase II study on stereotactic body radiotherapy for stage I non-small cell lung cancer. *Radiother Oncol* 2007;85:429–34.
42. Fakiris AJ, McGarry RC, Yiannoutsos CT, Papiez L, Williams M, Henderson MA, et al. Stereotactic body radiation therapy for early-stage non-small-cell lung carcinoma: four-year results of a prospective phase II study. *Int J Radiat Oncol Biol Phys* 2009;75:677–82.
43. Ricardi U, Filippi AR, Guarneri A, Giglioli FR, Ciammella P, Franco P, et al. Stereotactic body radiation therapy for early stage non-small cell lung cancer: results of a prospective trial. *Lung Cancer* 2010;68:72–7.
44. Kopek N, Paludan M, Petersen J, Hansen AT, Grau C, Høyer M. Co-morbidity index predicts for mortality after stereotactic body radiotherapy for medically inoperable early-stage non-small cell lung cancer. *Radiother Oncol* 2009;93:402–7.
45. Wulf J, Haedinger U, Oppitz U, Thiele W, Mueller G, Flentje M. Stereotactic radiotherapy for primary lung cancer and pulmonary metastases: a noninvasive treatment approach in medically inoperable patients. *Int J Radiat Oncol Biol Phys* 2004;60:186–96.
46. Okunieff P, Petersen AL, Philip A, Milano MT, Katz AW, Boros L, et al. Stereotactic body radiation therapy (SBRT) for lung metastases. *Acta Oncol* 2006;45:808–17.
47. Hof H, Hoess A, Oetzel D, Debus J, Herfarth K. Stereotactic single-dose radiotherapy of lung metastases. *Strahlenther Onkol* 2007;183:673–8.
48. Norihisa Y, Nagata Y, Takayama K, Matsuo Y, Sakamoto T, Sakamoto M, et al. Stereotactic body radiotherapy for oligometastatic lung tumors. *Int J Radiat Oncol Biol Phys* 2008;72:398–403.
49. Kim MS, Yoo SY, Cho CK, Yoo HJ, Choi CW, Seo YS, et al. Stereotactic body radiation therapy using three fractions for isolated lung recurrence from colorectal cancer. *Oncology* 2009;76:212–9.

Int. J. Radiation Oncology Biol. Phys., Vol. ■, No. ■, pp. 1–7, 2010

0360-3016/$–see front matter

ELSEVIER

doi:10.1016/j.ijrobp.2010.05.046

PHYSICS CONTRIBUTION

POSITIONAL REPRODUCIBILITY OF PANCREATIC TUMORS UNDER END-EXHALATION BREATH-HOLD CONDITIONS USING A VISUAL FEEDBACK TECHNIQUE

MITSUHIRO NAKAMURA, PH.D.,* KEIKO SHIBUYA, M.D., PH.D.,* TAKEHIRO SHIINOKI, M.S.,† YUKINORI MATSUO, M.D., PH.D.,* AKIRA NAKAMURA, M.D.,* MANABU NAKATA, R.T.T.,‡ AKIRA SAWADA, PH.D.,* TAKASHI MIZOWAKI, M.D., PH.D.,* AND MASAHIRO HIRAOKA, M.D., PH.D.*

*Department of Radiation Oncology and Image-applied Therapy, Graduate School of Medicine, Kyoto University, Kyoto, Japan; †Department of Nuclear Engineering, Graduate School of Engineering, Kyoto University, Kyoto, Japan; and ‡Clinical Radiology Service Division, Kyoto University Hospital, Kyoto, Japan

Purpose: To assess positional reproducibility of pancreatic tumors under end-exhalation (EE) breath-hold (BH) conditions with a visual feedback technique based on computed tomography (CT) images.
Methods and Materials: Ten patients with pancreatic cancer were enrolled in an institutional review board-approved trial. All patients were placed in a supine position on an individualized vacuum pillow with both arms raised. At the time of CT scan, they held their breath at EE with the aid of video goggles displaying their abdominal displacement. Each three-consecutive helical CT data set was acquired four times (sessions 1–4; session 1 corresponded to the time of CT simulation). The point of interest within or in proximity to a gross tumor volume was defined based on certain structural features. The positional variations in point of interest and margin size required to cover positional variations were assessed.
Results: The means ± standard deviations (SDs) of intrafraction positional variations were 0.0 ± 1.1, 0.1 ± 1.2, and 0.1 ± 1.0 mm in the left-right (LR), anterior-posterior (AP), and superior-inferior (SI) directions, respectively (p = 0.726). The means ± SDs of interfraction positional variations were 0.3 ± 2.0, 0.8 ± 1.8, and 0.3 ± 1.8 mm in the LR, AP, and SI directions, respectively (p = 0.533). Population-based margin sizes required to cover 95th percentiles of the overall positional variations were 4.7, 5.3, and 4.9 mm in the LR, AP, and SI directions, respectively.
Conclusions: A margin size of 5 mm was needed to cover the 95th percentiles of the overall positional variations under EE–BH conditions, using this noninvasive approach to motion management for pancreatic tumors. © 2010 Elsevier Inc.

Pancreatic cancer, Breath-hold, Visual feedback technique, Reproducibility, Internal margin.

INTRODUCTION

Pancreatic cancer is the fifth leading cause of cancer-related deaths in Japan. According to vital population statistics published by the Ministry of Health, Labor, and Welfare of Japan (1), pancreatic cancer resulted in approximately 25,960 deaths in 2008, and the number of people dying from pancreatic cancer is increasing year by year. Worldwide, in 2002, there were an estimated 232,000 new cases of pancreatic cancers and 227,000 deaths (2). Most patients present with locally advanced, unresectable, or metastatic disease at diagnosis (3). Locally advanced unresectable diseases without distant metastases are often treated with radiotherapy (RT), with or without concurrent chemotherapeutic agents, but the outcome is still modest.

Although recent developments of new drugs are remarkable and seem promising as systemic therapy, local persistence of disease remains serious. However, the prescribed doses in most previous studies had been limited to <60 Gy with conventional techniques (4–8), because the pancreatic tumor is adjacent to organs at risk (OARs), with lower tolerances for radiation, such as the stomach and duodenum. Thus, how to deliver more intensive RT while

Reprint requests to: Mitsuhiro Nakamura, Ph.D., Graduate School of Medicine, Kyoto University, Kyoto, 54 Kawahara-cho, Shogoin, Sakyo-ku, Kyoto 606-8507, Japan. Tel: (+81)-75-751-3762; Fax: (+81)-75-771-9749; E-mail: m_nkmr@kuhp.kyoto-u.ac.jp

This study was supported in part by a Grant-in-Aid for Scientific Research from the Ministry of Education, Culture, Sports, Science, and Technology of Japan (Grant no. 20229009), a Grant-in-Aid for Cancer Research (no. 20S-5) from the Ministry of Health, Labor, and Welfare of Japan, and a Grant-in-Aid for Scientific Research from the Association for Nuclear Technology in Medicine.This work was presented at the 51st Annual Meeting of the American Society for Radiation Oncology, Chicago, IL, Nov 1–5, 2009.

Conflicts of interest: none.

Received Nov 17, 2009, and in revised form May 24, 2010. Accepted for publication May 25, 2010.

minimizing the discontinuation of chemotherapy might become a greater issue for the treatment of pancreatic cancer. Both stereotactic body RT and intensity-modulated RT (IMRT) have the potential to safely escalate the radiation dose for pancreatic tumors without increasing toxicity to OARs.

Several investigators have quantified the intrafraction movement of pancreatic tumors under free breathing by using various modalities (9–15). Recently, Feng *et al.* (14) found that motion of the borders of pancreatic tumors was highly variable among patients, using cine magnetic resonance images, and reported that a margin of 20 mm inferiorly was required to provide 99% geometric coverage. Mori *et al.* (15) verified a gross tumor volume (GTV) displacement of >10 mm in the superior-inferior (SI) direction, with a 256-multislice four-dimensional computed tomography (CT) scanner. Thus, larger internal margins (IMs) are needed to fully cover geometric changes under free breathing (16). Consequently, a large volume of OARs will be included in a planning target volume.

The breath-hold (BH) technique reduces the impact of respiratory motion and has been applied successfully in treatment of lung and liver cancer patients (17–22). Our group has also shown that higher stability of the pancreatic tumor position was observed at end exhalation (EE) than at end-inhalation (23). Thus, we hypothesized that IMRT in combination with EE–BH might be a reliable method for achieving dose escalation for locally advanced pancreatic cancer with small margins. In order to accurately perform IMRT in combination with EE–BH, it is important to understand positional variations in pancreatic tumors under EE–BH conditions through the course of treatment (24); however, there have been few studies of this.

The purpose of this study was to assess the positional reproducibility of pancreatic tumors under EE–BH conditions with a visual feedback technique, based on CT images, and to calculate the margin size necessary to cover positional variations during the course of treatment.

METHODS AND MATERIALS

Patients

The eligibility criteria for this study were as follows: (*a*) patients who underwent RT in combination with chemotherapy for locally advanced pancreatic cancer; (*b*) patients whose performance status was scored 0 or 1; (*c*) patients who were able to hold their breath at EE for >15 sec; and (*d*) patients who provided written informed consent. Ten consecutive patients who met the above criteria were enrolled in this institutional review board-approved trial between January 2009 and October 2009. Six patients were treated with RT for 3 weeks, and 4 patients were treated with RT for 6 weeks. Patient characteristics are shown in Table 1.

A brochure explaining BH–CT scanning was distributed to all participating patients on the day before CT simulation. This brochure contained an illustration of a BH–CT scan using video goggles (iWear VR920; Vuzix Corporation, Rochester, NY).

Breath-hold helical CT scan

At the time of CT simulation (session 1), all patients were placed in a supine position on an individualized vacuum pillow (BodyFix; Medical Intelligence, Schwabmünchen, Germany) with both arms raised. A marker block with two infrared reflecting dots was placed tightly on the anterior abdominal surface of the patient (Fig. 1). Anterior-posterior (AP) abdominal skin surface displacement was monitored by a Real-time Positioning Management (RPM) system (Varian Medical Systems, Palo Alto, CA). A visual feedback technique was applied with the aid of video goggles displaying the abdominal displacement acquired by the RPM system. The patients were asked to breathe following simple audio instructions, such as "breathe in, breathe out, and hold your breath," and then held their breath at EE for >15 sec, depending on their ability, while watching their abdominal displacement with the goggles. They practiced until they held their breath successfully, which took around 5 min.

Table 1. Patient characteristics

Patient	Sex	Age (y)	Body weight (kg)	TNM	Location
1	F	76	46.8	T4N0M0	Body
2	F	72	59.7	T4N0M0	Body
3	M	44	90.3	T4N0M0	Body
4	M	72	61.9	T4N0M0	Body
5	M	66	65.7	T4N0M0	Head
6	M	58	65.6	T3N0M1*	Head
7	M	66	66.0	T4N0M0	Body
8	F	61	58.5	T3N0M1*	Tail
9	M	66	56.9	T4N0M0	Head
10	M	66	68.5	T4N0M0	Head

Abbreviations: M = male; F = female.
* Distant lymph node metastasis.

All participating patients stopped oral intake except for drugs and water for >3 hr before treatment planning and before each BH–CT scan. No patient was provided with oxygen at the BH–CT scan. The scan protocol at session 1 was as follows: before the BH–CT scan, two scout views were taken under EE–BH conditions to determine the scan start position. First, the whole abdomen, from the superior border of the liver to the iliac crest, was scanned with a four-slice CT scanner (LightSpeed RT; General Electric Medical Systems, Waukesha, WI) under EE–BH conditions with a visual feedback technique, which took around 30 sec. If the patient could not hold their breath for 30 sec at the time of practice, this scan was done twice with BH. The acquisition parameters of the helical CT scan were a rotational time of 1.0 sec and a helical pitch of 15

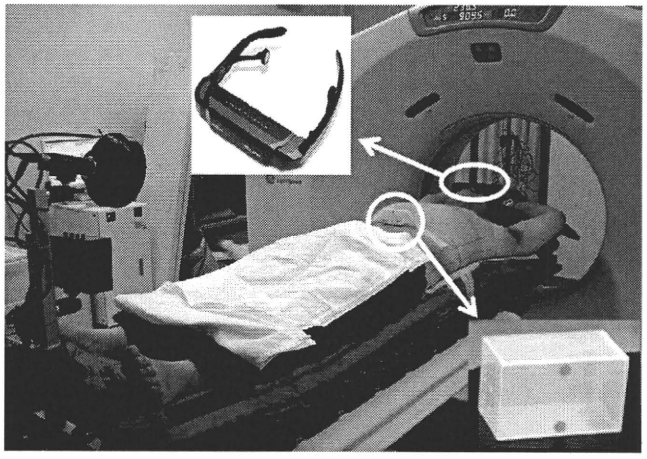

Fig. 1. Patient setup. All patients were placed in a supine position on an individualized vacuum pillow with both arms raised. A marker block (lower right) with two infrared reflecting dots was placed tightly on the anterior abdominal surface of the patient. Patients wore goggles (upper left) displaying the abdominal displacement.

mm/rotation. CT data were reconstructed in a field of view of 550 mm on a 512 × 512 grid with a slice thickness of 2.5 mm. Second, contrast-enhanced CT data were acquired with one EE–BH for approximately 200 mm centered on the pancreas, which took around 14 sec. Iodinated contrast medium , 300 mg/ml (25), was infused at a rate of 3 ml/sec (26). The patients received a total contrast medium volume based on twice their body weight (up to 100 ml) (27). The delay time between the injection of the contrast medium and the start of the contrast-enhanced BH–CT scan was set to 40 sec. Finally, another BH–CT scan was repeated promptly after the completion of the first contrast-enhanced BH–CT scan.

During the course of treatment, three consecutive BH–CT data sets were also acquired three times, at 1- to 2-min intervals, with no iodinated contrast medium (sessions 2–4). A scan range was approximately 200 mm, centered on the pancreas. Actual CT scan time was around 14 sec. The interval period between CT data acquisitions during the treatment course depended on the RT schedule (*i.e.*, once per week for patients who were treated with RT for 3 weeks and once per 2 weeks for those treated with RT for 6 weeks). Consequently, a total of 12 BH–CT data sets per patient were acquired.

Target definition

After the BH–CT scan, the point of interest (POI) within or in proximity to a GTV was defined by one radiation oncologist specializing in pancreatic cancer (K.S.), based on certain structural features that were not affected by the contrast medium, to detect, including calcification, points of disruption of the main pancreatic duct, points of adhesion of involved vessels within the tumor, or areas of low density within the tumor. The POIs for each session were determined without reference to POIs previously decided on a commercially available three-dimensional radiation treatment planning system (Eclipse, version 8.2; Varian Medical Systems). In this study, the GTV was not contoured to avoid geometric ambiguities that resulted from manual delineation (28).

Intra- and interfraction positional variations

Positional differences between the first POI and the two other POIs within each session were calculated to evaluate the intrafraction positional variations. In total, 80 values were analyzed in each direction.

Subsequently, positional differences between sessions (interfraction positional variations) were evaluated. Before calculating the interfraction positional variations, setup errors between the first BH–CT scan at session 1 and those at other sessions were corrected, based on the vertebral body, using the image registration algorithm of Eclipse. After image registration, alignment of the vertebral body around the pancreas was visually inspected by a medical physicist (M.N.). The registration was modified until the vertebral body misalignment was measured as <1.0 mm in any of the axial, coronal, and sagittal views. Following this, the interfraction positional variation was determined as the difference in the mean POI positions between session 1 and the three other sessions. In total, 30 values were acquired.

Internal margin sizes

To take into account the overall positional variations, both individual and population-based margin sizes were calculated. The individual margin sizes were defined as the maximum distance between the first POI position at session 1 and other POI positions. On the other hand, the population-based margin sizes were computed based on the linear sum of the standard deviation (SD) of the mean intrafraction positional variations (Σ_{intra}) and the root-mean-square of the individual SD in interfraction positional variations (σ_{inter}) (29). In this study, 95% confidence levels were chosen to calculate the population-based margin sizes. The value of the distribution associated with 95% nominal probability was 1.96. Then, an equation for the population-based margin calculation was expressed as $1.96 \times \Sigma_{intra} + 1.96 \times \sigma_{inter}$.

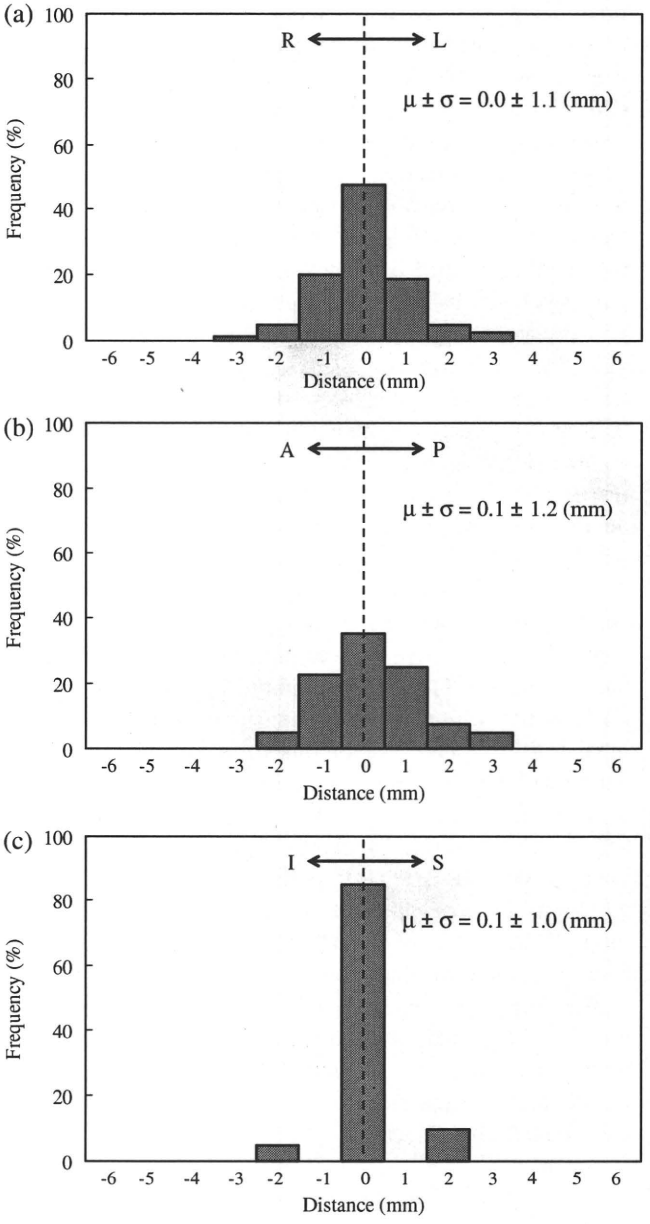

Fig. 2. Frequency distributions of the intrafraction positional variations. The means ± SDs were 0.0 ± 1.1, 0.1 ± 1.2, and 0.1 ± 1.0 mm in the (a) left-right, (b) anterior-posterior, and (c) superior-inferior directions, respectively.

Statistical analysis

One-way analysis of variance was performed to assess the significance of the positional variations among left-right (LR), AP, and SI directions. Values of $p < 0.05$ were deemed to indicate statistical significance.

RESULTS

All 10 patients were able to hold their breath at EE for around 20 sec, and 9 of 10 patients tolerated a BH of 30

sec, which was needed to scan the whole abdomen. The remaining 1 patient needed two scans to acquire the whole abdominal images. The decision of the POIs was not affected by the number of scans. The POIs were located based on calcification in 2 patients, points of disruption of the main pancreatic duct in 3 patients, points of adhesion of involved vessels within the tumor in 3 patients, and areas of low density within the tumor in 2 patients. Through repeated CT data acquisition, we did not have any patients in whom we could not identify each POI defined at session 1.

Intrafraction positional variations

Figure 2 shows the frequency distribution of the intrafraction positional variations. The means ± SDs of intrafraction positional variations were 0.0 ± 1.1 mm (range, −3.3 to 3.1 mm), 0.1 ± 1.2 mm (range, −2.5 to 3.3 mm), and 0.1 ± 1.0 mm (range, −2.5 to 2.5 mm) in the LR, AP, and SI directions, respectively. Positive values indicate the left, posterior, and superior directions. Among the 80 values, 55%, 46%, and 80% of the POI positions were reproducible to within the voxel size in the LR, AP, and SI directions, respectively. No significant difference was observed between the directions ($p = 0.726$).

Interfraction positional variations

A representative interfraction positional variation is shown in Fig. 3. The maximum positional difference was 5 mm in the SI direction. Figure 4 shows the frequency distributions of the interfraction positional variations. The means ± SDs of interfraction positional variations were 0.3 ± 2.0 mm (range, −3.5 to 4.5 mm), 0.8 ± 1.8 mm (range, −3.6 to 4.5 mm), and 0.3 ± 1.8 mm (range, −3.3 to 5.0 mm) in the LR, AP, and SI directions, respectively. The SDs of interfraction positional variations were larger than those of the intrafraction positional variation. Although larger systematic deviations were observed in the posterior than in other directions (Fig. 4), there were no significant differences between the directions ($p = 0.533$).

Internal margin sizes

The individual margin sizes to cover the overall positional variations are listed in Table 2. The maximum margin sizes were 5.5, 5.8, and 5.0 mm in the LR, AP, and SI directions, respectively. The margin size of 5 mm was sufficient to cover the overall positional variations in 7 of 10 patients.

The values of Σ_{intra} and σ_{inter} were 1.1 mm and 1.3 mm, 1.2 mm and 1.5 mm, and 1.0 mm and 1.5 mm in the LR, AP, and SI directions, respectively. Therefore, the population-based margin sizes of 4.7, 5.3, and 4.9 mm were calculated in the LR, AP, and SI directions, respectively. As setup correction was applied based on bony anatomy, these margins did not include the setup errors.

DISCUSSION

We evaluated positional variations in pancreatic tumors in 10 patients under EE–BH conditions, with a visual feedback technique based on CT images. None of the patients took anything orally except for drugs or water for >3 hr prior to treatment planning and each BH–CT scan. BH–CT scans were taken several minutes apart and repeated on different days. The POIs within or in proximity to a GTV were determined to quantify the positional variations after setup errors were corrected by matching bony anatomy. Under such conditions, we found that the margin size of 5 mm was needed to cover the 95th percentiles of the overall positional variations under EE–BH conditions.

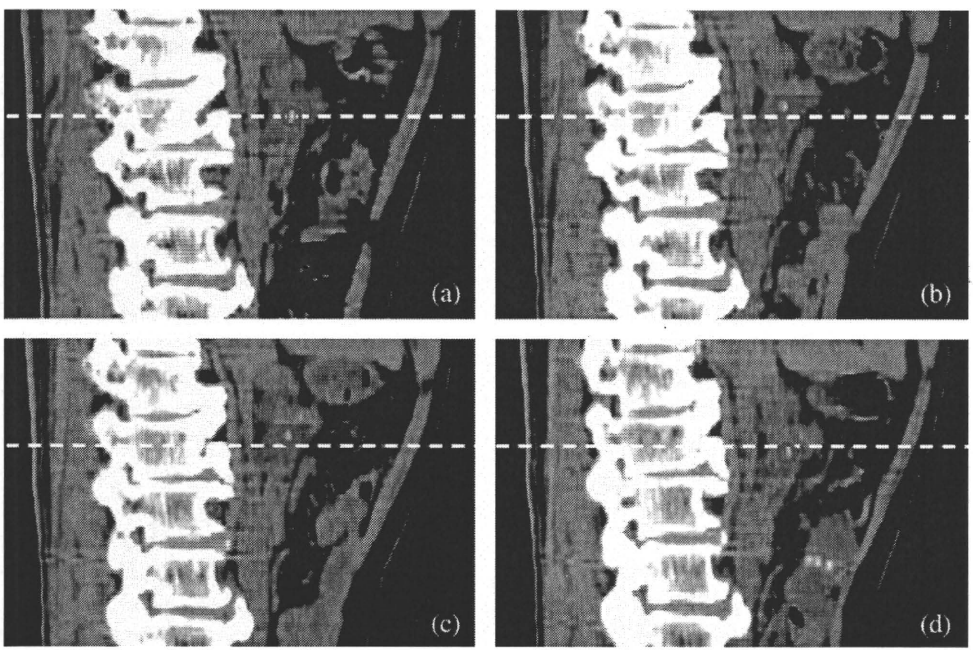

Fig. 3. Sagittal images at (a) session 1, (b) session 2, (c) session 3, and (d) session 4 for patient 6. An area of calcification was set as a point of interest (POI). White dashed lines show the mean POI position in the superior–inferior direction at session 1. The POI of each session is indicated by a red circle.

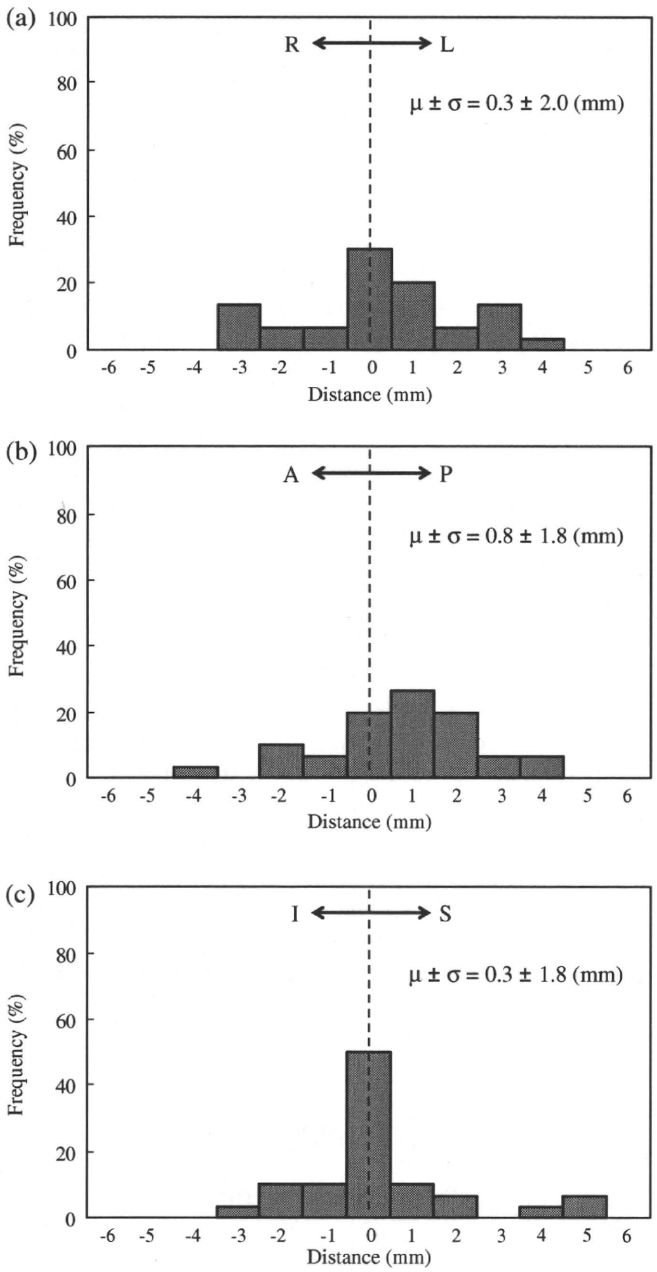

Fig. 4. Frequency distributions of the interfraction positional variations. The means ± SDs were 0.3 ± 2.0, 0.8 ± 1.8, and 0.3 ± 1.8 mm in the (a) left–right, (b) anterior–posterior, and (c) superior–inferior directions, respectively.

In the current study, the GTV itself was not delineated because the tumor border was less clear on CT images without the iodinated contrast medium. The variability of GTV delineation has been described for pancreatic tumors by Yamazaki *et al.* (28). The GTV centroid depended on the GTV size and shape in each CT slice. Our POI approach was adopted to focus on the accuracy of the positional variations.

According to a report published by the American Association of Physicists in Medicine (AAPM) (30), there are several approaches with regard to BH techniques. One is active breath control (ABC), developed at William Beaumont Hospital. Several investigators have shown the high reproducibility of ABC at various phases of the breathing cycle for

Table 2. Individual margin sizes

Patient	LR (mm)	AP (mm)	SI (mm)
1	4.6	5.8	0.0
2	3.9	4.1	2.5
3	2.8	2.0	2.5
4	3.3	3.8	0.0
5	1.8	1.9	2.5
6	2.5	2.0	5.0
7	1.8	4.1	0.0
8	5.3	1.9	2.5
9	5.5	5.0	2.5
10	4.5	2.1	5.0

Abbreviations: LR = left-right; AP = anterior-posterior; SI = superior-inferior.

patients with lung and liver cancer (17–19). The second technique is the voluntary deep-inspiration BH, with a commercially available spirometer. Hanley *et al.* (20) have indicated that intra-BH reproducibility of the lung tumor was 1.0 ± 0.9 mm. Their results were consistent with those of Mah *et al.* (21). The third technique is the BH method with no respiratory monitoring. Onishi *et al.* (22) have reported that the differences in lung tumor position were 2.2 ± 1.1 mm in the SI direction under patients' self-estimated breath-holding, with no respiratory monitoring. In the present study, the intrafraction positional variations were normally distributed, with a focus on the first POI within each session (Fig. 2). Unlike the three BH approaches described above, our BH maneuver was based on a visual feedback technique. In general, visual feedback improves the reproducibility of the abdominal wall, chest wall, and lung tumor positions (31–36). This visual feedback BH technique appeared to be effective in controlling the reproducibility of pancreatic tumor positions.

Wysocka *et al.* (37) have reported interfraction positional variations in the pancreas in voluntary expiration BH and showed that the 90th percentiles of the interfraction positional variations were 8.9, 7.9, and 23 mm in the LR, AP, and SI directions, respectively (37). Our results for interfraction positional variations were more favorable than the results of their study (Fig. 4). The visual feedback technique may also help to reduce the interfraction positional variation. In addition to respiratory movement, a possible cause of the interfraction positional variations in pancreatic tumors involves anatomical characteristics. Pancreatic tumors are surrounded by flexible structures, such as the stomach, small intestine, and colon. During the course of treatment, some patients experience anorexia and suffer from digestive troubles. Gastrointestinal states, including gastrointestinal content and bowel gas, generally vary with time because of physiological phenomena and some digestive disorders (Fig. 5). These changes in gastrointestinal states might affect pancreatic tumor positions.

We acquired a total of 12 BH–CT data sets per patient, not only at the time of CT simulation but also during the course of treatment, and found that the pancreatic tumor position was not always reproducible at the position at the time of CT simulation, even under EE–BH conditions. This finding is important in determining the margin size for IMRT in

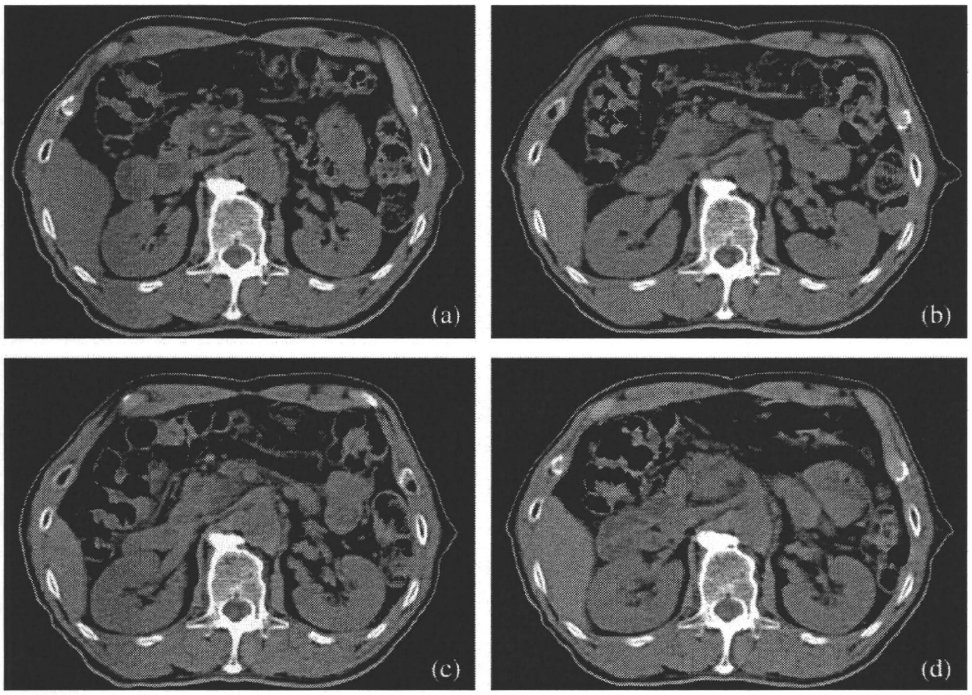

Fig. 5. Axial images at (a) session 1, (b) session 2, (c) session 3, and (d) session 4 for patient 6. An area of calcification was set as a point of interest (POI). The POI is indicated by a red circle (a). These images display the same axial position. States in bowel vary with time.

combination with EE–BH. Report 62 of the International Commission on Radiation Units and Measurements recommends that a clinical target volume should be enlarged with an IM to compensate for the effects of physiological changes, as well as target motion during the administration of radiotherapy (16). AAPM Report 91 also indicates that interfraction positional variation does occur and should be considered (30). This means that an appropriate IM size cannot be decided based on only one CT scan. Although Murphy *et al.* (38) indicated that pancreatic tumor position in three dimensions was reproducible to within 2.5 mm at end-inhalation, based on implanted gold fiducials, our study showed that margin sizes of 2.5 mm were insufficient to encompass the overall positional variations (Table 2). From the results of 12 BH–CT scans, it was found that a margin size of 5 mm was needed to cover the 95th percentiles of the overall positional variations under EE–BH conditions.

The IMRT technique typically uses 5 to 7 ports to deliver the entire prescribed set of monitor units (MUs), and one set of MUs in one port can be delivered in 15 sec EE–BH using the highest dose rate (600 MU/min in our machine). Thus, the number of BH times that corresponds to the number of ports is required for one fraction. As can be estimated from Fig. 2, the impact of the intrafraction positional variations on dose distribution is considered nonsignificant within one fraction. Rather, interfraction positional variations could have an effect on dose distribution. The effect, however, can be minimized by adding margin sizes to encompass the interfraction positional variations. Thus, a margin size of 5 mm plus the setup margin will ensure that the planned dose is delivered to the target volumes. Also, the visual feedback BH technique provided significant margin reduction, compared with the results of the studies under free breathing (14, 15), which will reduce the incidence of high-grade gastrointestinal toxicity (39).

CONCLUSIONS

Positional variations in pancreatic tumors were assessed under EE–BH conditions with a visual feedback technique, based on CT images. The intrafraction positional variations were mostly slight. A margin size of 5 mm was needed to cover the 95th percentiles of the overall positional variations under EE–BH conditions using this noninvasive approach to motion management for pancreatic tumors.

REFERENCES

1. CANCER STATISTICS IN JAPAN '09 institution: National Cancer Center topic title: Number of Death, by Cancer Site (2007), and Mortality Rate by Cancer Site (2007). http://ganjoho.jp/public/statistics/backnumber/2009_en.html. Last accessed August 27, 2010.
2. Parkin DM, Bray F, Ferlay J, *et al.* Global cancer statistics, 2002. *CA Cancer J Clin* 2005;55:74–108.
3. Warshaw AL, Fernandez-del CC. Pancreatic carcinoma. *N Engl J Med* 1992;326:455–465.
4. Moertel CG, Childs DS Jr., Reitemeier RJ, *et al.* Combined 5-fluorouracil and supervoltage radiation therapy of locally unresectable gastrointestinal cancer. *Lancet* 1969;2:865–867.
5. Moertel CG, Frytak S, Hahn RG, *et al.* Therapy of locally unresectable pancreatic carcinoma: a randomized comparison of

high dose (6,000 rads) radiation alone, moderate dose radiation (4000 rads + 5-fluorouracil), and high dose radiation + 5-fluorouracil: The Gastrointestinal Tumor Study Group. *Cancer* 1981; 48:1705–1710.
6. Klaassen DJ, MacIntyre JM, Catton GE, *et al.* Treatment of locally unresectable cancer of the stomach and pancreas: A randomized comparison of 5-fluorouracil alone with radiation plus concurrent and maintenance 5-fluorouracil–an Eastern Cooperative Oncology Group study. *J Clin Oncol* 1985;3:373–378.
7. Treatment of locally unresectable carcinoma of the pancreas: Comparison of combined-modality therapy (chemotherapy plus radiotherapy) to chemotherapy alone. Gastrointestinal Tumor Study Group. *J Natl Cancer Inst* 1988;80:751–755.
8. Loehrer PJ, Powell ME, Cardenes HR, *et al.* A randomized phase III study of gemcitabine in combination with radiation therapy versus gemcitabine alone in patients with localized, unresectable pancreatic cancer: E4201. *J Clin Oncol* 2008;26: 4506.
9. Bryan P, Custar S, Haaga J, *et al.* Respiratory movement of the pancreas: An ultrasonic study. *J Ultrasound Med* 1984;3:317–320.
10. Suramo I, Paivansalo M, Myllyla V. Cranio-caudal movements of the liver, pancreas and kidneys in respiration. *Acta Radiol Diagn (Stockh)* 1984;25:129–131.
11. Davies SC, Hill AL, Holmes RB, *et al.* Ultrasound quantitation of respiratory organ motion in the upper abdomen. *Br J Radiol* 1994;67:1096–1102.
12. Gierga DP, Chen GTY, Kung JH, *et al.* Quantification of respiration-induced abdominal tumor motion and its impact on IMRT dose distributions. *Int J Radiat Oncol Biol Phys* 2004;58:1584–1595.
13. Bussels B, Goethals L, Feron M, *et al.* Respiration-induced movement of the upper abdominal organs: a pitfall for the three-dimensional conformal radiation treatment of pancreatic cancer. *Radiother Oncol* 2003;68:69–74.
14. Feng M, Balter JM, Normolle D, *et al.* Characterization of pancreatic tumor motion using cine MRI: surrogates for tumor position should be used with caution. *Int J Radiat Oncol Biol Phys* 2009;74:884–891.
15. Mori S, Hara R, Yanagi T, *et al.* Four-dimensional measurement of intrafractional respiratory motion of pancreatic tumors using a 256 multi-slice CT scanner. *Radiother Oncol* 2009;92:231–237.
16. International Commission on Radiation Units and Measurements. Prescribing, recording and reporting photon beam therapy, ICRU report no. 62 (Supplement to ICRU Report No. 50). Bethesda, MD: ICRU; 1999.
17. Wong JW, Sharpe MB, Jaffray DA, *et al.* The use of active breathing control (ABC) to reduce margin for breathing motion. *Int J Radiat Oncol Biol Phys* 1999;44:911–919.
18. Dawson LA, Brock KK, Kazanjian S, *et al.* The reproducibility of organ position using active breathing control (ABC) during liver radiotherapy. *Int J Radiat Oncol Biol Phys* 2001;51: 1410–1421.
19. Koshani R, Balter JM, Hayman JA, *et al.* Short-term and long-term reproducibility of lung tumor position using active breathing control (ABC). *Int J Radiat Oncol Biol Phys* 2006;65:1553–1559.
20. Hanley J, Debois MM, Mah D, *et al.* Deep inspiration breath-hold technique for lung tumors: the potential value of target immobilization and reduced lung density in dose escalation. *Int J Radiat Oncol Biol Phys* 1999;45:603–611.
21. Mah D, Hanley J, Rosenzweig KE, *et al.* Technical aspects of the deep inspiration breath-hold technique in the treatment of thoracic cancer. *Int J Radiat Oncol Biol Phys* 2000;48:1175–1185.
22. Onishi H, Kuriyama K, Komiyama T, *et al.* A new irradiation system for lung cancer combining linear accelerator, computed tomography, patient self-breath-holding, and patient-directed beam-control without respiratory monitoring devices. *Int J Radiat Oncol Biol Phys* 2003;56:14–20.
23. Shiinoki T, Narita Y, Nakamura M, *et al.* Analyses of interfractional variations in pancreatic position based on four-dimensional computed tomography. *Int J Radiat Oncol Biol Phys* 2009;75:S578.
24. Jiang SB, Wolfgang J, Mageras GS. Quality assurance challenges for motion-adaptive radiation therapy: Gating, breath holding, and four-dimensional computed tomography. *Int J Radiat Oncol Biol Phys* 2008;71:S103–S107.
25. Fenchel S, Fleiter TR, Aschoff AJ, *et al.* Effect of iodine concentration of contrast media on contrast enhancement in multislice CT of pancreas. *Br J Radiol* 2004;77:821–830.
26. Yamashita Y, Komahara Y, Takahashi M, *et al.* Abdominal helical CT: evaluation of optimal doses of intravenous contrast material: A prospective randomized study. *Radiology* 2000; 216:718–723.
27. Kim T, Murakami T, Takahashi S, *et al.* Pancreatic CT imaging: Effect of different injection rates and doses of contrast material. *Radiology* 1999;212:219–225.
28. Yamazaki H, Nishiyama K, Tanaka E, *et al.* Dummy run for a phase II multi-institute trial of chemoradiotherapy for unresectable pancreatic cancer: interobserver variance in contour delineation. *Anticancer Res* 2007;27:2965–2971.
29. Mckenzie AL. How should breathing motion be combined with other errors when drawing margins around clinical target volumes? *Br J Radiol* 2000;73:973–977.
30. Keall PJ, Mageras GS, Balter JM, *et al.* The management of respiratory motion in radiation oncology report of AAPM Task Group 76. *Med Phys* 2006;33:3874–3900.
31. Kubo HD, Wang L. Introduction of audio gating to further reduce organ motion in breathing synchronized radiotherapy. *Med Phys* 2002;29:345–350.
32. Kini VR, Vedam SS, Keall PJ, *et al.* Patient training in respiratory-gated radiotherapy. *Med Dosim* 2003;28:7–11.
33. Carlson SK, Felmlee JP, Bender CE, *et al.* Intermittent-mode CT fluoroscopy-guided biopsy of the lung or upper abdomen with breath-hold monitoring and feedback: System development and feasibility. *Radiology* 2003;229:906–912.
34. Nelson C, Starkschall G, Balter P, *et al.* Respiration-correlated treatment delivery using feedback-guided breath hold: A technical study. *Med Phys* 2005;32:175–181.
35. George R, Chung TD, Vedam SS, *et al.* Audio-visual biofeedback for respiratory-gated radiotherapy: Impact of audio instruction and audio-visual biofeedback on respiratory-gated radiotherapy. *Int J Radiat Oncol Biol Phys* 2006;65:924–933.
36. Nakamura K, Shioyama Y, Nomoto S, *et al.* Reproducibility of the abdominal and chest wall position by voluntary breath-hold technique using a laser-based monitoring and visual feedback system. *Int J Radiat Oncol Biol Phys* 2007;68:267–272.
37. Wysocka B, Kassam Z, Lockwood G, *et al.* Interfraction and respiratory organ motion during conformal radiotherapy in gastric cancer. *Int J Radiat Oncol Biol Phys* 2010;77:53–59.
38. Murphy JD, Martin D, Whyte R, *et al.* The effectiveness of breath-holding to stabilize lung and pancreas tumors during radiosurgery. *Int J Radiat Oncol Biol Phys* 2002;53:475–482.
39. Murphy JD, Adusumilli S, Griffith KA, *et al.* Full-dose gemcitabine and concurrent radiotherapy for unresectable pancreatic cancer. *Int J Radiat Oncol Biol Phys* 2007;68:801–808.